R. & M. No. 3209

MINISTRY OF AVIATION

AERONAUTICAL RESEARCH COUNCIL
REPORTS AND MEMORANDA

An Experimental Investigation of the Transonic Flow over an Unswept Wing of Aspect Ratio 3·5, Taper Ratio 0·5, with a 4 per cent Biconvex Section

By

J. B. Scott-Wilson, M.A.

LONDON : HER MAJESTY'S STATIONERY OFFICE
1961
PRICE 12*s.* 6*d.* NET

An Experimental Investigation of the Transonic Flow over an Unswept Wing of Aspect Ratio 3·5, Taper Ratio 0·5, with a 4 per cent Biconvex Section

By

J. B. SCOTT-WILSON, M.A.

COMMUNICATED BY THE PRINCIPAL DIRECTOR OF SCIENTIFIC RESEARCH (AIR), MINISTRY OF SUPPLY

Reports and Memoranda No. 3209

November, 1955

Summary.—The results of force measurements and surface oil flow studies on a wing-body combination with an unswept wing of aspect ratio 3·5, taper ratio 0·5, and a 4 per cent biconvex section, are analysed. The tests were made at Mach numbers from 0·72 to 1·02, at a Reynolds number of $1·89 \times 10^6$. At four Mach numbers, 0·70, 0·80, 0·93 and 0·96, a picture of the flow development with incidence is built up, based on the oil flow patterns on the wing, and a correlation is established between changes in overall forces, and changes in the flow development. At other Mach numbers the flow development is inferred from the overall forces by means of this correlation, and, in this way, an attempt is made to show how transonic flow develops over the wing.

At transonic Mach numbers four phases in the development of the flow with incidence are found. These are (*a*), no shock-induced separation, (*b*), shock-induced separation, with the shock roughly stationary on the wing, (*c*), shock-induced separation, with a rapid forward movement of the shock, and (*d*), leading edge separation. The aerodynamic derivatives are found to assume roughly constant values in each phase, and their variation with phase and Mach number is considered.

1. *Introduction.*—During recent years knowledge of the transonic behaviour of two-dimensional aerofoils has been considerably extended by the work of Pearcey and others at the National Physical Laboratory[1, 2]. Their work has shown that on two-dimensional aerofoils the rate of development of local regions of supersonic flow, terminated by shock waves, can be profoundly affected by the interaction of the shock waves with the wing boundary layer. When the incidence of a thin aerofoil is increased at a fixed transonic Mach number, the terminating shock on the upper surface moves rearward, and increases in strength, until its strength is sufficient to separate the wing boundary layer. This separation forms a small bubble on the wing and reduces the pressure recovery through the shock wave. Pearcey has shown that if the incidence is further increased until the pressure recovery is insufficient to re-establish subsonic conditions after the shock, there is a rapid expansion of the separation bubble towards the trailing edge. At this stage in the flow development the trailing-edge pressure falls rapidly and the rearward movement of the upper surface shock is halted. With any further increase in incidence the upper surface shock moves forward towards the leading edge.

No such detailed information exists on the development of transonic flow over unswept wings of finite aspect ratio. A certain amount of information on the variation of overall aerodynamic characteristics of finite unswept wings at transonic speeds is now available from the results of tests in American high-speed and transonic tunnels[3, 4] and from tests on freely

falling models[5]. In Ref. 6 some pressure distributions on an aspect ratio 4 wing with a 4 per cent biconvex section are given for Mach numbers from 0·6 to 1·05. In none of these cases has an attempt been made to build up a picture of development of the overall flow field.

Recently, as part of a research programme in the 3 ft × 3 ft Wind Tunnel at the National Aircraft Establishment, Bedford, on the aerodynamic characteristics of wing-body combinations at transonic and supersonic speeds, three wings of aspect ratio 3·5, taper ratio 0·5, with an unswept half-chord line, have been tested. Three different wing sections were used for these models, a 6 per cent RAE 104 section, a 4 per cent RAE 104 section and a 4 per cent biconvex section. The lift, drag, and pitching moment results on these wings at transonic speeds and at supersonic speeds up to $M = 1{\cdot}82$, have recently been presented, without analysis[7]. In this note, the transonic results for the 4 per cent biconvex wing are considered in more detail. The oil flow technique, described in Ref. 8, has been used to indicate the occurrence and the extent of shock induced, or leading-edge separations, and to show the approximate position of shock waves on the wing. At four Mach numbers changes in the oil flow patterns are correlated with characteristic changes in the overall force data. From this correlation an attempt is made to describe the complete development of the flow over the wing from $M = 0{\cdot}70$ to $M = 1{\cdot}02$.

2. *Results of 3 ft × 3 ft Wind Tunnel Tests on the 4 per cent Biconvex Wing.*—The general arrangement and principal dimensions of the wing-body combination model with 4 per cent biconvex section wings are given in Fig. 1. This model was mounted on a sting in the 3 ft × 3 ft Wind Tunnel, and the overall forces on the model measured using an internal strain-gauge balance. A fuller description of the experimental technique is given in Ref. 7. The measured lift, drag, and pitching-moment coefficients are shown in Figs. 2 to 5. Fig. 2 shows the variation of lift coefficient, C_L, with incidence, α, through the Mach number range, Fig. 3 the variation of pitching-moment coefficient, C_m, with lift coefficient, C_L, Fig. 4 the variation of drag coefficient, C_D, with lift coefficient, C_L, Fig. 6 the variation of C_D with C_L^2. The pitching-moment coefficient is referred to the quarter-chord point of the aerodynamic mean chord. The Mach number range covered was from $M = 0{\cdot}70$ to $M = 1{\cdot}02$, and all tests were made at a Reynolds number, based on aerodynamic mean chord, of $1{\cdot}89 \times 10^6$. All the force measurements presented in Figs. 2 to 5 were obtained with transition fixed by a band of distributed roughness from 0 to 10 per cent chord on each surface. The importance of fixing transition, when testing unswept wings at transonic speeds, will be discussed in a later report on these tests.

The oil flow patterns were obtained by covering the wings with a thin film of a mixture of heavy oil and titanium oxide, and then, with the model at the required incidence, running the tunnel at constant Mach number until the pattern developed. Since this technique was briefly described in Ref. 8, it has been developed for use with the transonic working section, which is not fitted with windows. By using a consistently thin film of oil, and by running the tunnel to a predetermined time schedule, satisfactory oil flow patterns have been obtained without a constant visual check on their development. In these tests no pressure measurements were taken, so that it is not possible to correlate the oil flow patterns with pressure distributions. Such a correlation has however been made in tests on a 60 deg swept wing reported in Ref. 9. In the majority of oil flow tests, patterns have been obtained with transition fixed on one wing, and free on the other, enabling both cases to be examined in one run.

The flow patterns and force measurements obtained at Mach numbers of 0·70, 0·80, 0·93 and 0·96, are examined in detail. A brief examination is also made of the flow patterns obtained at a constant incidence of 8·8 deg, as the Mach number varied from 0·85 to 1·02. An overall assessment of the flow development in the transonic range $M = 0{\cdot}70$ to $M = 1{\cdot}02$ is made in Section 3.

2.1. *Results for a Range of Incidence at $M = 0{\cdot}70$.*—Two oil flow patterns were obtained on the upper surface of the wing at $\alpha = 4{\cdot}3$ deg, and $\alpha = 6{\cdot}5$ deg, at $M = 0{\cdot}70$, and are shown in Fig. 6. At $\alpha = 4{\cdot}3$ deg it appears that the wing boundary layer separates at the leading edge of the wing, and re-attaches to the wing surface farther aft at about 35 per cent chord.

The ' long bubble ' of separated flow, so formed, is shown by the patch of unmoved oil in the photograph. At 6·5 deg incidence the bubble appears to extend to about 80 per cent chord over the central section of the wings. Flow inside the bubble, forward towards the leading edge, is shown near the tips in the oil flow patterns at this incidence. The development of a long bubble of separated flow is typical of subsonic flow over thin wings at incidence. Previous investigations, such as Ref. 10, have shown that the chordwise extent of a long bubble increases with incidence in a similar manner to the bubble on this wing, and that finally a stage is reached in the flow development where the long bubble extends beyond the trailing edge. A new feature of the three-dimensional bubbles observed here is that they do not extend unchanged into the wing root and up to the tip but that their length decreases and is practically zero at either end.

Another feature of the flow, indicated by the oil flow patterns, is the development of marked tip vortices, such as have been considered by Küchemann in Refs. 11 and 12. The outward flow of oil in a triangular region at the tip suggests that the tip vortex sheet curves in over the upper surface of the wing, and winds up with the centre of the spiral just inboard of the tip. Air drawn by the vortex sheet down onto the wing surface and then under the core would leave this characteristic oil flow pattern.

The aerodynamic characteristics of the wing at $M = 0{\cdot}70$, previously shown in Figs. 2 to 5, have been replotted in Fig. 7, for comparison with the oil flow patterns, as the variation of C_L, C_m, and $C_D - (K_A/\pi A)C_L^2$, with incidence. K_A is the overall drag factor for small incidences, and has a value of 1·79. Non-linear variations of the drag are emphasised by presenting the drag results in this way.

The lift-curve slope shows a slight increase in slope with incidence up to about $\alpha = 5$ deg, but as the incidence is increased further, the lift-curve slope falls off, gradually up to about $\alpha = 7$ deg, and then more rapidly. The non-linear increase in lift at low incidence is consistent with the effect of tip vortices on lift, predicted by Küchemann in Ref. 11. The long bubble appears to have little effect on lift while the bubble is closed onto the wing surface well forward of the trailing edge, as is the case at $\alpha = 4{\cdot}3$ deg. However, as the long bubble approaches the trailing edge the lift-curve slope decreases. By comparing these results with those in Ref. 6, where pressure measurements have been taken, it appears that as the long bubble extends towards the trailing edge the pressure there begins to fall, and this in turn causes a reduction in the pressures on the lower surface. This reduction in lower surface pressures will contribute to the decrease in lift-curve slope under these conditions.

The pitching-moment curve shows a linear variation of C_m with α up to about 5 deg incidence, beyond which there is a continuous gain in stability, here assessed in terms of $\partial C_m/\partial\alpha$. Correlating this curve with the flow development shown by the oil flow patterns, it appears that the long bubble has no effect on the stability of the wing until it extends close to the wing trailing edge.

The drag curve shows non-linear drag effects at incidences above 3 deg. As it has been shown in Ref. 11 that tip vortices do not affect the drag to a first order, it would appear that the long bubble causes an increase in drag at a very early stage in its development, which can probably be attributed to the loss of the leading-edge suction force in association with non-linear lift forces.

2.2. *Results for a Range of Incidence at $M = 0{\cdot}80$.*—The four oil flow pictures in Fig. 8 show the flow patterns that were obtained on the upper surface of the wing at incidences of 4·4 deg, 5·5 deg, 6·6 deg and 7·6 deg at $M = 0{\cdot}80$. At 4·4 deg incidence the flow no longer separates from the leading edge to form a long bubble, as is the case at $M = 0{\cdot}70$, but is attached to the surface up to the main wing shock, which appears from the flow pattern to be at about 15 per cent chord over the central section of the wing. On the wing with fixed transition the shock appears to cause a small separation bubble about 20 per cent chord in length. The bubble is indicated by a region of unmoved oil, in the picture, and the shock is assumed to be at the upstream edge

of this region. On the wing with free transition the shock appears to cause only a very small bubble, shown by the piling up of oil along the shock line. On this wing transition occurs very close to the leading edge, and there appears to be a trace of oil left unmoved right at the leading edge. This suggests that the laminar boundary layer separates at the leading edge, but re-attaches very shortly afterwards as a turbulent boundary layer. Tip vortices can again be seen in the flow pattern.

At 5·5 deg incidence, interpreting the flow pattern in a similar way, the shock has moved back to about 19 per cent chord. On both wings there is a bubble of separated flow behind the shock. The bubble extends about 25 per cent chord on the wing with transition fixed, and about 10 per cent chord on the wing with transition free. The shock moves back only slightly between 5·5 deg and 6·6 deg incidence, but the separation bubble behind the shock increases in length, which is doubled by 6·6 deg.

Between 6·6 deg and 7·6 deg incidence there is a major change in the flow pattern. Although at 7·6 deg incidence shock separation still appears to occur over the outer part of the span on the wing with transition fixed, over the inner part of the span the flow appears to separate from the leading edge, as the only movement of oil apparent in this region is forward towards the leading edge. On the wing with transition free, the flow appears to separate at the leading edge over the whole span, and except in the tip regions where air is drawn onto the wing surface by the tip vortices, remains separated over the entire upper wing surface. Because of the considerable buffeting of the model, and the large rolling moments occurring between 6·6 deg and 7·6 deg incidence, it is believed that the change-over from flow attached at the leading edge with shock induced separation farther aft, to flow separated at the leading edge, takes place suddenly rather than as a gradual development with the shock moving forward to the leading edge.

The force data for the model at $M = 0{\cdot}80$ is shown in Fig. 9. The lift curve slope shows the same non-linear increase in lift at small angles of incidence as the curve for $M = 0{\cdot}70$, and this is again probably caused by the formation of strong tip vortices. Beyond 5 deg incidence, as the separation bubble behind the shock spreads towards the trailing edge the lift curve slope decreases. There appears to be no very abrupt loss of lift at the change from shock-induced separation to leading edge separation.

The pitching-moment curve shows a slight decrease in stability with increase in incidence up to about $\alpha = 5$ deg. In the absence of a transonic theory for the flow over such a wing, it is not certain to what extent this loss in stability is due to the development of the potential field, or how much is due to viscous effects. Further light may be shed on this when the results of two-dimensional transonic tests at N.P.L. on the 4 per cent biconvex section become available. Between $\alpha = 5$ deg and $\alpha = 7$ deg, in the region where the separation bubble is expanding, there is a gradual gain in stability. A much more marked gain in stability occurs as the change to leading-edge separation takes place.

The overall drag factor, K_A, was found to be 1·82 for this Mach number. The curve in Fig. 9 shows that $C_D - (K_A/\pi A)C_L^2$ is constant up to 5·5 deg incidence, but rises rapidly as the incidence is further increased.

2.3. *Results for a Range of Incidence at* $M = 0{\cdot}93$.—The flow patterns on the wing at $M = 0{\cdot}93$ are shown in Fig. 10. Oil flow patterns have been obtained on the upper surface of the wing for incidences of 0·0, 2·2, 4·5, 8·8, 11·0 and 11·9 deg. The general basis of interpretation of these patterns is similar to that at $M = 0{\cdot}80$. Where areas of separated flow shown by unmoved regions of oil occur on the wing surface it is assumed that they are caused by shocks at their upstream edge. At zero incidence there is no flow separation. Transition occurs very close to the leading edge on the wing with transition free, and the pattern is rather underdeveloped towards the trailing edge of this wing. At 2·2 deg incidence the only development that can be detected in the oil flow pattern is the formation of tip vortices. However, by 4·5 deg incidence the main wing shock, at about 75 per cent chord, has become

strong enough to separate the wing boundary layer. Because this shock is now far back on the wing, the separation bubble does not close on the wing, as was the case at $M = 0{\cdot}80$, but must extend beyond the trailing edge almost as soon as it is formed. By $8{\cdot}8$ deg incidence the main wing shock has moved forward to about 45 per cent chord. The flow pattern for $\alpha = 8{\cdot}8$ deg shows that two oblique shocks form on the wing, one from the root leading edge, and the other from the tip leading edge. They appear in the oil pattern as lines at which the oil streaks change direction. The occurrence and the effect of these shocks will be discussed further in Section 3.1, but it can be seen from the oil flow patterns that they limit the spanwise extent of the main wing recompression shock. Faint traces of these shocks can also be seen in the patterns at $\alpha = 4{\cdot}4$ deg. By 11 deg the shock has moved forward to about 30 per cent chord. The pattern on the wing with transition fixed is rather underdeveloped at this incidence. At $11{\cdot}9$ deg the flow fails to attach at the leading edge on the wing with transition fixed. On the wing with transition free, the flow is still attached up to the shock at about 30 per cent chord. Oil flow patterns have also been obtained on the lower surface of the wing at these incidences, but in no case is shock separation indicated.

The measured force data for the wing at $M = 0{\cdot}93$ is shown in Fig. 11. The lift-curve slope again shows a marked non-linear increase in lift between 0 and 3 deg. At 3 deg incidence, where shock-induced separation probably occurs, the lift-curve slope starts to decrease again. Between 5 deg and $11{\cdot}5$ deg incidence, roughly the range of incidence for which the shock moves forward towards the leading edge, the lift-curve slope is approximately constant at a value well below that at $C_L = 0$. Finally at about $11{\cdot}5$ deg there is a sudden loss of lift, which suggests that at this incidence there is an abrupt change from shock-induced separation at about 30 per cent chord, as indicated in the flow pattern at $11{\cdot}0$ deg, to a leading-edge separation, as indicated in the pattern for $11{\cdot}9$ deg.

The pitching-moment curve shows a slight loss in stability between 0 and 2 deg incidence. Between 2 and 4 deg incidence there is a marked gain in stability, which may result from the onset of shock separation and also from the tip vortex sheets. As the shock moves forward on the wing there is first a slight loss in stability, from $\alpha = 5$ deg to $\alpha = 8$ deg, followed by a steady gain in stability. There is no marked change in pitching moment when the sudden loss in lift, corresponding to the change to leading-edge separation, occurs.

The overall drag factor, K_A, was found to be $1{\cdot}14$ for small incidences. The onset of separation at about 3 deg incidence leads to a rapid non-linear rise of the drag.

2.4. *Results for a Range of Incidence at* $M = 0{\cdot}96$.—The oil flow patterns, obtained on the upper surface of the wing at $M = 0{\cdot}96$, are shown in Fig. 12. The incidences at which patterns have been obtained, are $0{\cdot}0$, $2{\cdot}2$, $4{\cdot}5$, $6{\cdot}7$, $8{\cdot}9$, $10{\cdot}0$ and $12{\cdot}2$ deg. At small incidences the flow patterns are similar to those obtained at $M = 0{\cdot}93$. The shock separation again occurs between $2{\cdot}2$ and $4{\cdot}5$ deg incidence, but the shock in this case is farther aft at about 85 per cent chord. In contrast to its behaviour at $M = 0{\cdot}93$, the shock at $M = 0{\cdot}96$ does not move forward rapidly with increase in incidence, once separation has occurred, but stays well back on the wing, and becomes considerably distorted over the inner and outer parts of the wing, where it is influenced by the oblique shocks from root and tip leading edges. At $6{\cdot}7$ deg the shock is still at 85 per cent chord, except near the tips where it moves back to the trailing edge. At $8{\cdot}9$ deg incidence the shock is at about 75 per cent chord over the middle part of the wing, but moves back to about 90 per cent chord near the root, and to the trailing edge near the tip. At 10 deg incidence the shock has moved forward to 70 per cent chord over the middle part of the wing, but is still severely distorted in the root and tip regions. At $12{\cdot}2$ deg the shock is at about 50 per cent chord, and extends almost in to the wing root. The two oblique shocks still exist, but their influence is much more restricted at this incidence. From the force curves in Fig. 2 it can be seen that the loss in lift associated with the change to a leading edge separation, occurs at $14{\cdot}2$ deg incidence. The flow patterns on the lower surface at these incidences again gave no indication of shock separation.

The measured force data for $M = 0{\cdot}96$ is shown in Fig. 13. The lift curve again shows a non-linear increase in lift with incidence up to about $\alpha = 3$ deg. The loss in lift-curve slope above 3 deg incidence is not so large in this case as at $M = 0{\cdot}93$, and the slope becomes roughly constant between $\alpha = 4$ deg and $\alpha = 9$ deg, the range of incidence for which the shock is well back on the wing, at about the same value as at $C_L = 0$. A further decrease in lift-curve slope takes place beyond $\alpha = 10$ deg, as the shock moves forward on the wing.

The pitching-moment curve shows a slight loss in stability from $\alpha = 0$ deg to $\alpha = 2$ deg, but where shock separation occurs, between $\alpha = 2$ deg and $\alpha = 4$ deg, there is a large increase in stability. The stability parameter, $\partial C_m/\partial\alpha$, is roughly constant from $\alpha = 4$ deg to $\alpha = 9$ deg, at a much more stable value than was the case in this incidence range at $M = 0{\cdot}93$. The forward movement of the shock, between $\alpha = 10$ deg and $\alpha = 12$ deg is again associated with a loss in stability.

The overall-drag factor, K_A, was found to be $1{\cdot}36$ at small incidences at $M = 0{\cdot}96$. The onset of shock induced separation again leads to a non-linear increase in overall drag. A comparison of the $C_D - (K_A/A\pi)C_L^2$ curves for $M = 0{\cdot}96$, and $M = 0{\cdot}93$ shows that the non-linear effects are similar up to about 4 deg incidence, but that beyond 4 deg incidence a much more rapid increase in non-linear drag occurs at $M = 0{\cdot}93$ than at $M = 0{\cdot}96$.

2.5. *Flow Patterns at* $8{\cdot}8$ *deg Incidence for a Range of Mach Number.*—A series of oil flow patterns have been obtained for the wing at Mach numbers from $M = 0{\cdot}85$ to $M = 1{\cdot}02$ at a constant nominal incidence of 8 deg; the true incidence, due to the deflection of the sting, varies from $8{\cdot}7$ deg at $M = 0{\cdot}85$ to $8{\cdot}9$ deg at $M = 1{\cdot}02$. These patterns, shown in Fig. 14, are interpreted in a similar way to those in the preceding sections. At $M = 0{\cdot}85$ on the wing with transition fixed, the flow has separated from the leading edge over the inner two thirds of the span. Close to the tip the flow appears to be attached at the leading edge, and separated at a shock at about 25 per cent chord. On the wing with transition free there is a shock separation at about 30 per cent chord. When the Mach number reaches $0{\cdot}90$ the flow is attached at the leading edge on both wings but separates at the shock at about 30 per cent to 35 per cent chord. With increase in Mach number the shock moves back on the wing, reaching 45 per cent chord at $M = 0{\cdot}93$, and 75 per cent chord at $M = 0{\cdot}96$. At $M = 0{\cdot}96$, as was noted in the previous Section, the shock is considerably distorted by the effects of the two oblique shocks from root and tip leading edges. At $M = 0{\cdot}99$, and $M = 1{\cdot}02$, the oblique shocks dominate the flow pattern, and only in a small region at their intersection is the flow separated. The angle of the oblique shocks appears to be independent of Mach number in this range. This suggests that the angle depends primarily on the local Mach number ahead of the shock, for Pearcey[1] has shown that at fixed incidence in two-dimensions the local Mach number is independent of free-stream Mach number at transonic speed.

3. *The Development of Transonic Flow over the Wing.*—In the preceding sections, a picture of the flow development with incidence, at four Mach numbers, has been built up based on the oil flow patterns. Comparing the measured forces with this physical picture, characteristic changes in the forces have been shown to occur at definite stages in the flow development. Because of the lack of a potential transonic theory, it is not possible to predict the characteristics of the wing in the absence of boundary-layer separation, and without this standard of comparison, the changes in overall forces that seem to occur when the flow separates, cannot with certainty be attributed to the effects of separation. However, the consistent correlation between changes in force measurements and changes in flow pattern at these four Mach numbers suggests that the flow development at other Mach numbers can be inferred from changes in overall forces alone. An attempt will be made, using this correlation, to show how transonic flow develops over the wing.

Once local supersonic regions, terminated by shock waves, appear on the wing, the development of the flow, as the incidence is increased at constant Mach number, can be split up into four phases. Phase A covers the low incidence range, in which, although shock waves

exist on the wing, they are of insufficient strength to separate the wing boundary layer. This is followed by phase B, a range of incidence for which shock separation occurs, but the shock remains roughly stationary on the wing. The third phase C covers the incidence range where rapid forward movement of the shock occurs. This is succeeded by phase D, the high incidence range in which the flow fails to attach at the leading edge. The boundaries between phases A, B and C, cannot be precisely defined because the development of shock separation takes place gradually and the phases tend to merge into each other. The boundary between phases C and D is defined more exactly as there is a sudden change from shock separation to leading-edge separation.

The approximate boundaries between the phases have been determined, for the range of Mach number covered, by an examination of the measured force data. These boundaries are shown in terms of C_L in Fig. 15. The boundary between phases A and B, the point at which shock separation occurs, has been taken as the approximate value of C_L at which the lift curve has an inflexion, non-linear drag effects become apparent, and a nose-down change in stability occurs. With the boundary defined in this way, cases, such as $\alpha = 4{\cdot}4$ deg and $\alpha = 5{\cdot}5$ deg at $M = 0{\cdot}80$, where the separation bubble is closed on the wing well forward of the trailing edge, are included in phase A. The boundary between phases B and C is more difficult to determine. The results at $M = 0{\cdot}93$ and $M = 0{\cdot}96$ have shown that the forward movement of the shock coincides with a decrease in stability. The boundary has therefore been taken as the value of C_L at which there is an inflexion of the C_m vs. C_L curves in Fig. 3. There is also reasonable agreement between this point and the second break in the C_D vs. C_L^2 curves in Fig. 5. The boundary between phases C and D is taken as the maximum value of C_L before the sudden loss in lift, associated with the change from shock induced separation to leading-edge separation, occurs. The boundary at $M = 0{\cdot}80$, where this sudden loss in lift does not occur, cannot be determined in this way, and an approximate value of C_L, based on the assessment of the oil flow patterns in Section 2.2, has been used.

The phase boundaries in Fig. 15 show that shock separation effects first influence the flow over the wing at a Mach number of about $0{\cdot}75$, and that as the Mach number increases they play a more and more dominant part in the development of the flow. The shock separation boundary between phases A and B decreases progressively from a C_L of $0{\cdot}47$ at $M = 0{\cdot}80$ until it levels off at a C_L of $0{\cdot}22$ at $M = 0{\cdot}99$. The boundary between phases B and C increases slightly with Mach number up to $M = 0{\cdot}85$, and then falls to a C_L of $0{\cdot}37$ at $M = 0{\cdot}93$. At $M = 0{\cdot}96$ the C_L range covered by phase B becomes greatly increased in extent, and phase C does not begin until a C_L of $0{\cdot}84$ is reached. Phase B in this case includes the incidence range in which the main wing shock is considerably distorted by the influence of the oblique shocks from the root and tip leading edges. At $M = 0{\cdot}99$ and $M = 1{\cdot}02$ the boundary between phases B and C lies at $C_L = 0{\cdot}96$. Possible reasons for the increased extent of phase B at these Mach numbers are considered in Section 3.1. The third boundary line, the value of C_L at which leading-edge separation occurs, rises with increasing Mach number from $C_L = 0{\cdot}48$ at $M = 0{\cdot}70$, where the approximate value of C_L at which the long bubble reaches the trailing edge has been taken, to $C_L = 1{\cdot}12$ at $M = 0{\cdot}96$. At $M = 0{\cdot}99$ and $M = 1{\cdot}02$ the change to leading-edge separation does not occur in the incidence range covered.

The variation of the main aerodynamic derivatives in the first three phases of the development of the flow is next examined. In most cases these derivatives are found to assume a roughly constant value for the major part of each phase. It is only where the phases are of very limited extent that the derivatives do not reach a steady value. Where possible the lift-curve slope, $\partial C_L/\partial\alpha$, the aerodynamic centre $\partial C_m/\partial C_L$, and the overall drag factor K, have been determined.

The variation of the lift-curve slope with Mach number in each phase is shown in Fig. 16. The variation of slope at $C_L = 0$ is shown for the whole range of Mach number. Because of the non-linear nature of the lift curve at small incidences, the slope has been taken between + 1 deg and − 1 deg. This curve shows the gradual rise in lift-curve slope with Mach number, up to $M = 1{\cdot}0$, that has been found in previous tests on straight wings of aspect ratio about three[3, 4, 5]. The reason for the irregular step at $M = 0{\cdot}93$ is not known. The second curve in Fig. 16 shows

the variation of lift-curve slope with Mach number in phase B. Because of the limited extent of this phase at Mach numbers below 0·96, the slope has only been determined for Mach numbers from 0·96 to 1·02. As mentioned in Section 2.4, the lift-curve slope in phase B has about the same value as at $C_L = 0$. In phase C where the shock is moving forward on the wing, the lift-curve slope is well below its zero-lift value. The curve showing the variation of $\partial C_L/\partial \alpha$ with Mach number in phase C has a marked peak at $M = 0{\cdot}93$.

The effect of shock separation on the aerodynamic centre, $\partial C_m/\partial C_L$, is shown in Fig. 17. At zero lift the aerodynamic centre remains constant at 10 per cent (measured from the leading edge) of the aerodynamic mean chord up to $M = 0{\cdot}90$, and then moves aft with increase in Mach number reaching 22·5 per cent aerodynamic mean chord by $M = 1{\cdot}02$. In contrast to the results of Ref. 3, there is no tendency for the aerodynamic centre to move forward at the lower transonic Mach numbers. Between $M = 0{\cdot}96$ and $M = 1{\cdot}02$ the aerodynamic centre in phase B is roughly constant at 35 per cent aerodynamic mean chord. The aerodynamic centre in phase C is also roughly constant at 25 per cent aerodynamic mean chord for Mach numbers from 0·85 to 0·96.

The zero-lift drag curve is shown in Fig. 18. The drag rise starts at a Mach number of about 0·91, and appears to be levelling off by $M = 1{\cdot}02$. The Mach number range covered is insufficient to find where the maximum value of C_{D0} occurs. The overall drag factors, K_A, K_B and K_C, corresponding to the three phases A, B and C, have been obtained from the C_D vs. C_L^2 curves in Fig. 5, and are shown in Fig. 19. K_A remains roughly constant at a value of 1·76 from $M = 0{\cdot}70$ to $M = 0{\cdot}90$, but then decreases to 1·14 at $M = 0{\cdot}93$ before rising again to a steady value of 1·48 at $M = 0{\cdot}99$. This type of variation of overall drag factor, with a minimum value in the transonic range, has been found in other tests on thin unswept wings[3,5]. K_B rises gradually from 1·76 at $M = 0{\cdot}80$ to 2·20 at $M = 0{\cdot}96$ and then remains constant. K_C however follows roughly the same variation with Mach number as K_A, but is about double the value.

These results in Figs. 16, 17 and 19 show that the values of the aerodynamic derivatives in each phase are grouped at roughly the same level for the Mach numbers where they have been determined, but that large differences in level occur from phase to phase. In passing from phase A to phase B there is little change in lift-curve slope, or increase in overall drag factor, but a large rearward movement of the aerodynamic centre. Between phases B and C there is a considerable decrease in lift-curve slope, an increase in overall drag factor, and a forward movement of the aerodynamic centre. At the boundary between phases C and D the wings stall, with a sudden loss of lift. Conditions beyond the stall have not been considered.

3.1. *The Development of Phase B at Mach Numbers between* 0·96 *and* 1·02.—In the preceding section it has been shown that at Mach numbers of 0·96 and above, phase B, where the shock remains roughly stationary on the wing, extends over a much greater range of C_L than is the case at lower Mach numbers. This change in the way the flow develops has a marked effect on the aerodynamic characteristics of the wing, in particular on the movement of the aerodynamic centre. The possibility that tunnel wall interference affects the flow development on the wing in these conditions cannot be excluded, but two further possible explanations why the shock remains far back on the wing will be considered. Either this effect may be a section characteristic, that could be investigated in two-dimensional tests, or it may be caused by the influence of the oblique shocks from root and tip leading edges. There is some evidence from Ref. 1 that this may be primarily a section effect. In Fig. 44 of that paper the movement of the upper-surface shock with change in incidence is shown for a 6 per cent RAE 104 section at various transonic Mach numbers. A very abrupt decrease in the rate of forward movement of the shock after separation, occurs between $M = 0{\cdot}85$ and $M = 0{\cdot}90$. A similar effect may be found to occur on the 4 per cent biconvex section between $M = 0{\cdot}93$ and $M = 0{\cdot}96$. The two oblique shocks from root and tip leading edges appear to correspond to the steep pressure rise in these regions, predicted by linearised theory at supersonic speeds. It seems probable from the oil flow patterns that these shocks are further strengthened by viscous effects. At the tip,

the tip vortex spreads inwards over the wing towards the trailing edge, as air from outside the tip is drawn into it. This vortex sheet, forming in effect an end plate, inclined slightly inwards, will force the upper surface air in towards the root. An oblique shock of increased strength may be necessary to turn the flow into the direction of this effective end-plate. The spread of air from the body onto the wing surface at the root, possibly accentuated by the presence of a root vortex[13], may strengthen the root shock in a similar way. The flow ahead of the shocks is inclined slightly in towards the body, because of the sweep of the leading edge. This will tend to strengthen the shock at the root, and weaken the shock at the tip. An indication of the probable strength of these shocks can be obtained from the pressure measurements in Ref. 6, where pressure ratios across the oblique shocks of about 1·25 were found. By providing part of the necessary total pressure recovery these oblique shocks will weaken the parts of the main wing recompression shock that lie within their regions of influence, and the distortion, shown in the oil flow patterns, will result. It is probable that the pressure in the separated flow behind the main wing shock in the central part of the wing, is also affected by conditions in the root and tip regions. This would influence the shock position, and may result in the shock remaining far back on the wing.

4. *Practical Implications.*—4.1. *Buffeting.*—No exact correlation yet exists between flight measurements of buffet boundaries and tunnel measurements of shock separation. It is suggested in Ref. 2 that buffeting may first occur when the separation bubble on the wing extends to the trailing edge. If this is the case, the buffet boundary for the wing tested will lie close to the boundary between phases A and B in Fig. 15. At constant Mach number the buffet intensity should remain at roughly the same level throughout phase B, because there is little change in the area of separated flow. With increase in Mach number, the area of separated flow in phase B decreases, as is shown in Figs. 14(d) to 14(f), and there may be some reduction in buffet intensity. Phase C covers a range of C_L in which the area of separated flow, and probably the buffet intensity increases rapidly. No definite conclusions can, however, be drawn at this stage and more work, including direct measurements of flow oscillations, is required.

4.2. *Stability Changes.*—In the preceding section the aerodynamic centre at any Mach number was shown to be roughly constant for the major part of each phase, but to vary considerably from one phase to the next. The phase boundaries in Fig. 15 will therefore represent the approximate values of C_L at which large changes in stability occur. Fig. 17 shows the order of this movement of aerodynamic centre.

4.3. *The Limit to Usable C_L.*—The boundary between phases C and D represents the maximum usable value of C_L that can be obtained from the wing without resort to noseflaps or other auxiliary devices. At this value of C_L the wing stalls, with a sudden loss in lift* and a large nose down change in pitching moment. Because of the sudden nature of the stall it is probable that wing dropping will occur. In practice, at the higher Mach numbers the severity of buffeting may prevent the attainment of this value of C_L.

5. *Conclusions.*—The results of overall force measurements and surface oil flow studies in the 3 ft Transonic Tunnel at the National Aircraft Establishment, Bedford, on a wing-body combination with an unswept wing of aspect ratio 3·5, taper ratio 0·5, and with a 4 per cent biconvex section, have been analysed. The tests were made at Mach numbers from 0·70 to 1·02 at a Reynolds number of $1·89 \times 10^6$. At four Mach numbers, 0·70, 0·80, 0·93 and 0·96, a picture of the flow development with incidence has been built up using the oil flow patterns on the wing, and a correlation has been established between changes in the overall forces and changes in the flow patterns. At other Mach numbers the flow development has been inferred from the overall forces, using this correlation, and, in this way, an attempt is made to show how transonic flow develops over the wing.

* Further increase with incidence to higher Values of C_L is still possible, however.

At transonic Mach numbers, four phases in the development of the flow with increasing incidence are found. The first phase covers the low incidence range, in which, although shock waves may exist on the wing, they are of insufficient strength to separate the wing boundary layer. This is followed by a second phase, in which shock separation takes place, but the shock remains roughly stationary on the wing. The third phase covers the incidence range where rapid forward movement of the shock occurs, and the last phase is the high incidence range where the flow separates at the leading edge.

Shock-induced separation first appears at a Mach number of about $0{\cdot}75$ and then occurs at progressively lower values of C_L as the Mach number increases; the variation is from a C_L of $0{\cdot}47$ at $M = 0{\cdot}80$ to a C_L of $0{\cdot}22$ at $M = 0{\cdot}99$, and $M = 1{\cdot}02$. The change to leading-edge separation occurs at higher values of C_L as the Mach number increases, varying from $C_L = 0{\cdot}52$ at $M = 0{\cdot}80$ to $C_L = 1{\cdot}12$ at $M = 0{\cdot}96$, the highest Mach number at which leading-edge separation is found in the incidence range covered. The second phase, where the shock remains roughly stationary on the wing, covers a very limited C_L range up to $M = 0{\cdot}93$, but for Mach numbers of $0{\cdot}96$ and above, this phase becomes a very significant one in the development of the flow. It is not certain whether this change in the flow development at $M = 0{\cdot}96$ is a section characteristic or whether it is a result of the oblique shocks from root and tip leading edges causing considerable distortion of the main wing shock at this Mach number.

The main aerodynamic derivatives, the lift-curve slope, the aerodynamic centre, and the drag factor, assume roughly constant values in each phase, but vary considerably from phase to phase. Shock separation, while the shock remains roughly stationary on the wing, causes little change in lift-curve slope or overall drag factor, but a large rearward movement of the aerodynamic centre. When the shock moves forward there is a marked decrease in lift-curve slope, a rise in the drag factor and a forward movement of the aerodynamic centre.

REFERENCES

No.	*Author*	*Title, etc.*
1	H. H. Pearcey	Some effects of shock-induced separation of turbulent boundary layers on transonic flow past aerofoils. N.P.L. Symposium on boundary layer effects in aerodynamics, Paper No. 9. March, 1955. R. & M. 3108. June, 1955.
2	D. W. Holder, H. H. Pearcey, G. E. Gadd and J. Seddon.	The interaction between shock waves and boundary layers, with a note on ' The effects of the interaction on the performance of supersonic intakes ". C.P. 180. February, 1954.
3	C. F. Hall	Lift, drag and pitching moment of low-aspect-ratio wings at subsonic and supersonic speeds. N.A.C.A. Research Memo. A53A30, NACA/TIB/3646. April, 1953.
4	J. L. Summers, S. L. Trean and L. A. Graham	Effects of taper ratio on the longitudinal characteristics at Mach numbers from 0·6 to 1·4 of a wing-body-tail combination having an unswept wing of aspect ratio 3. N.A.C.A. Research Memo. A54L20, NACA/TIB/4598. March, 1955.
5	M. D. White	A flight investigation at transonic speeds of the aerodynamic characteristics of a model having a thin unswept wing of aspect ratio 3·1. N.A.C.A. Research Memo. A54E12, NACA/TIB/4300. August, 1954.
6	G. Hieser, J. H. Henderson and J. M. Swihart	Transonic aerodynamic and load characteristics of a 4 per cent-thick unswept-wing-fuselage combination. N.A.C.A. Research Memo. L54B24, NACA/TIB/4242. May, 1954.
7	J. B. Scott-Wilson	The lift, drag and pitching moment of three unswept wings of aspect ratio 3·5, and taper ratio 0·5, with different wing sections at transonic and supersonic speeds. Unpublished M.o.A. Report.
8	K. G. Winter, J. B. Scott-Wilson and F. V. Davies.	Methods of determination, and of fixing boundary layer transition on wind tunnel models at supersonic speeds. C.P. 212. September, 1954.
9	F. O'Hara and J. B. Scott-Wilson	An investigation of the flow over a half-wing model with 60·5 degree leading edge sweepback at high subsonic and supersonic speeds. C.P. 471. November, 1955.
10	G. B. McCullough and D. E. Gault	Boundary layer and stalling characteristics of the N.A.C.A. 64A006 airfoil section. A.R.C. 12,781. August, 1949.
11	D. Küchemann	A non-linear lifting surface theory for wings of small aspect ratio with edge separations. A.R.C. 17,769. April, 1955.
12	D. Küchemann	Boundary layers on swept wings : Their effects and their measurement. Unpublished M.o.A. Report.
13	A. Stanbrook	Experimental observation of vortices in wing-body junctions. R. & M. 3114. March, 1957.

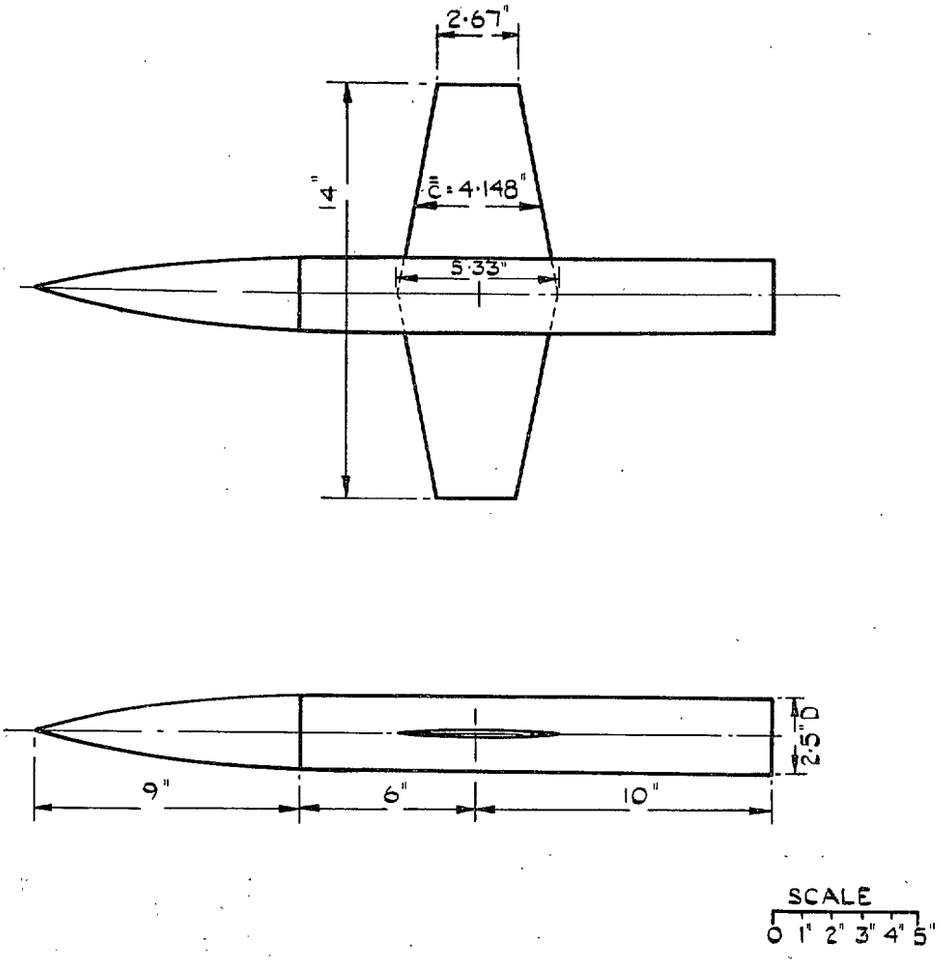

WING PLANFORM

ASPECT RATIO	3·5
TAPER RATIO	0·5
HALF CHORD SWEEP	0°

WING SECTION.

4 % BICONVEX SECTION

BODY PROFILE.

CYLINDRICAL WITH OGIVE NOSE

FIG. 1. Details of the model.

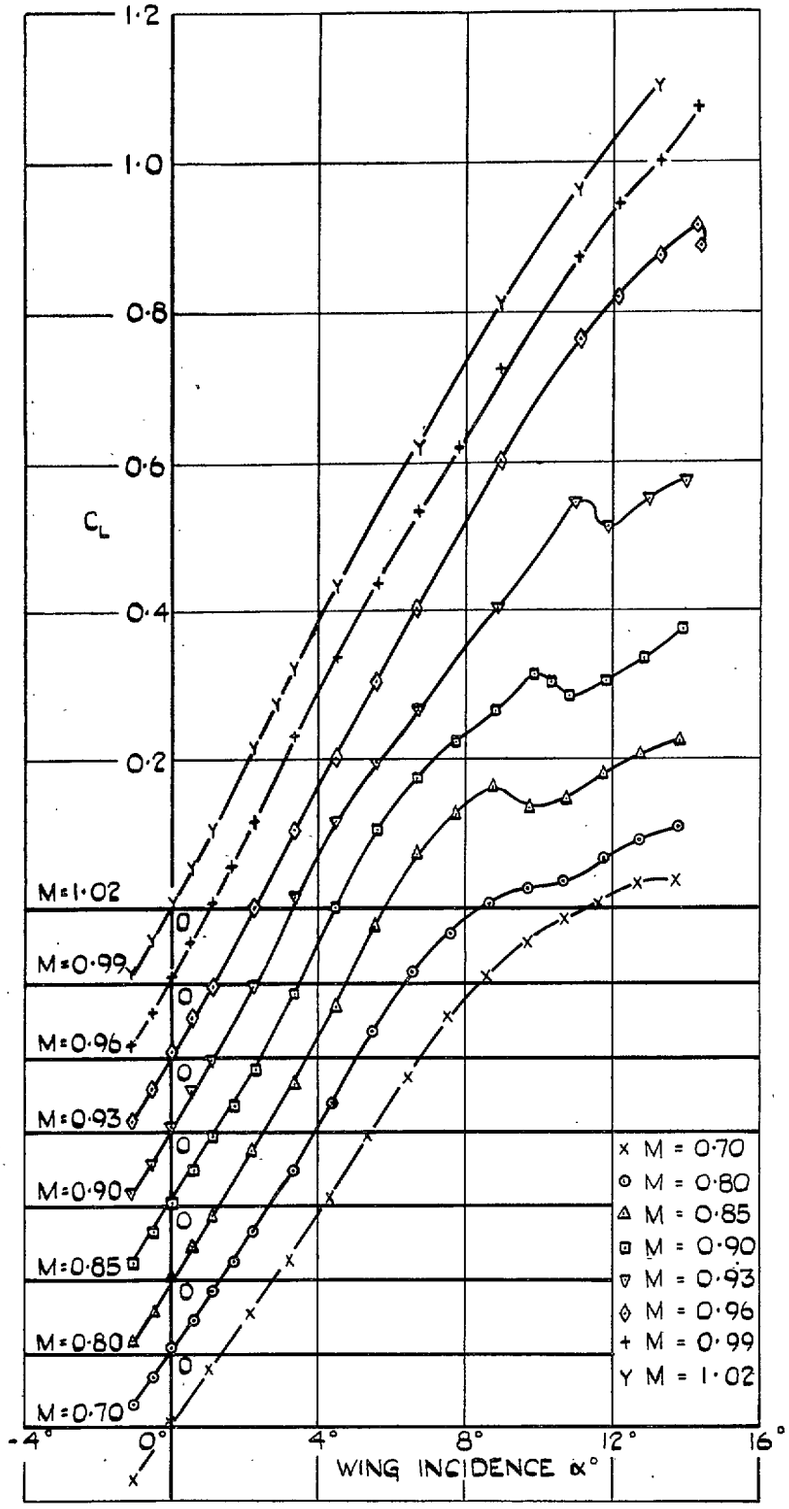

FIG. 2. The variation of lift coefficient, C_L, with wing incidence, α, through the Mach number range.

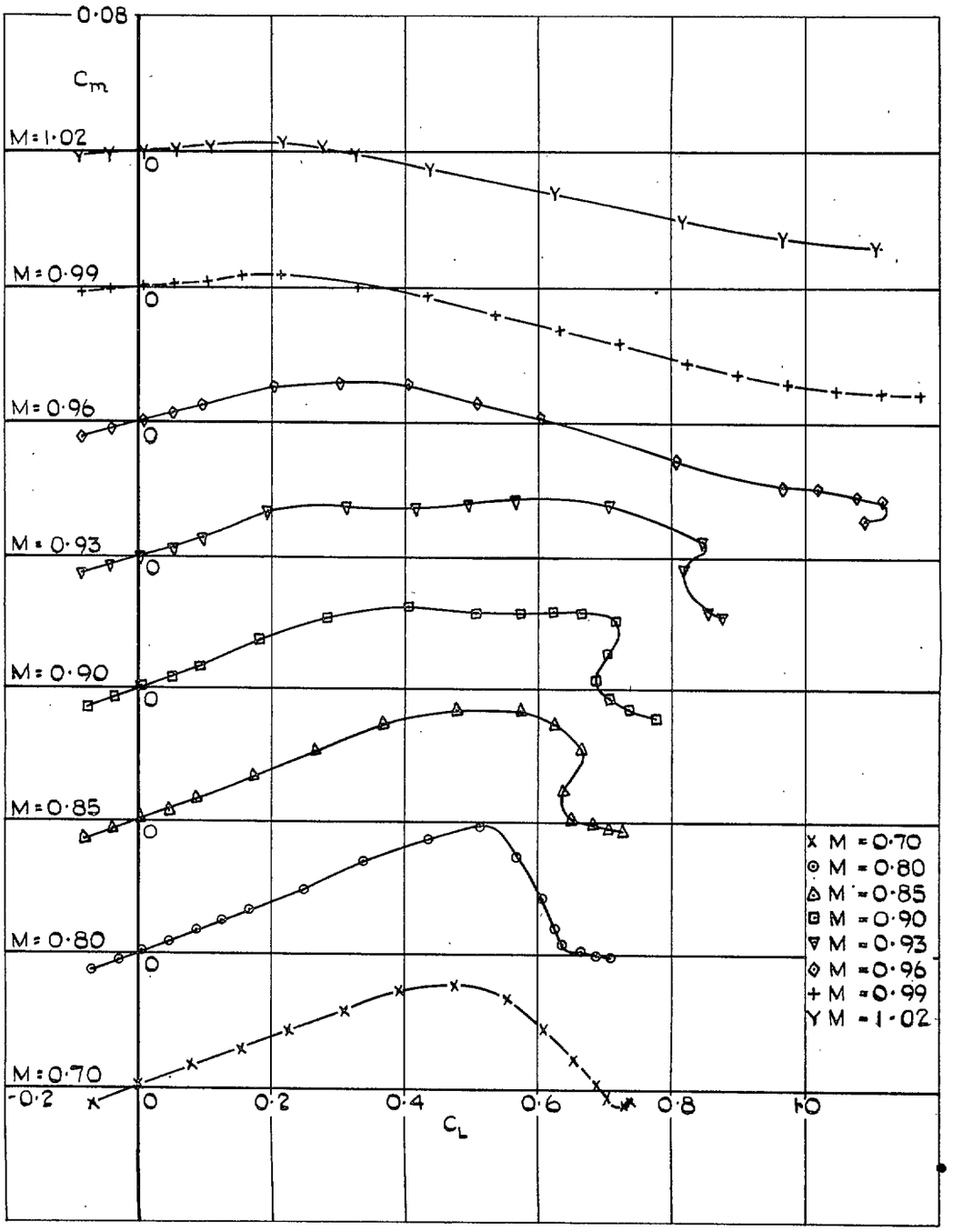

FIG. 3. The variation of pitching moment coefficient, C_m, with lift coefficient, C_L, through the Mach number range.

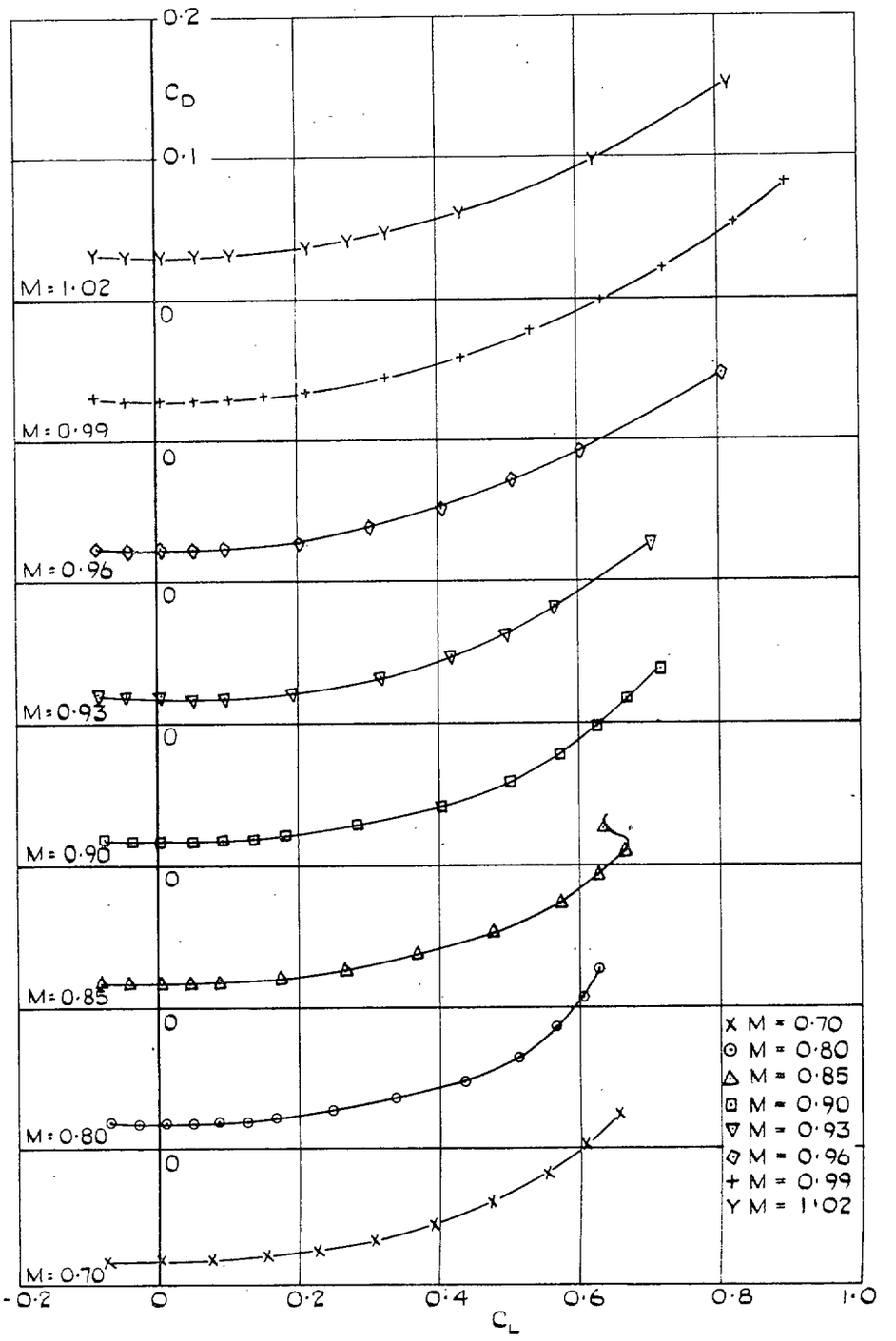

FIG. 4. The variation of C_D with C_L through the Mach number range.

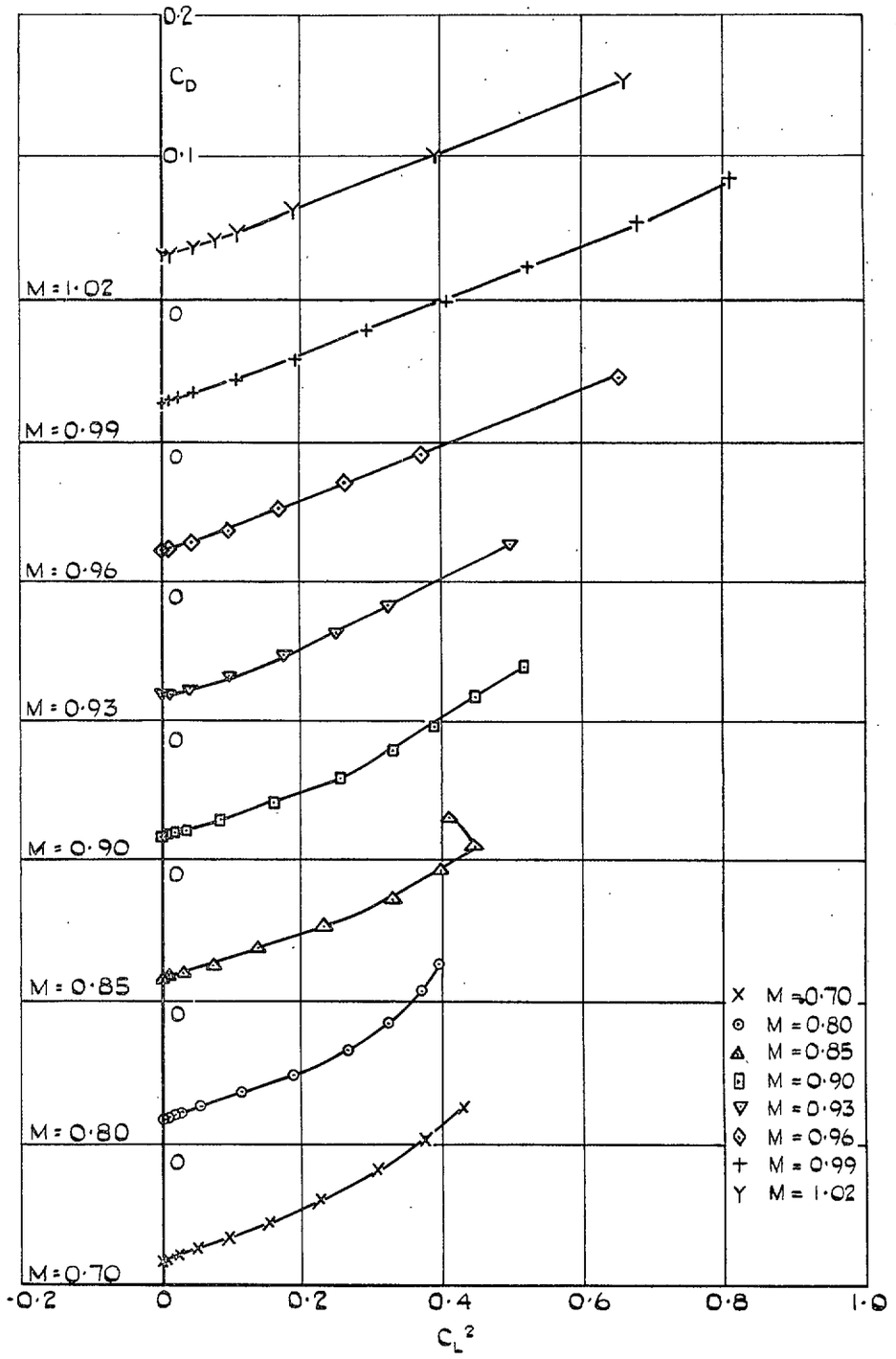

FIG. 5. Variation of C_D with C_L^2 through the Mach number range.

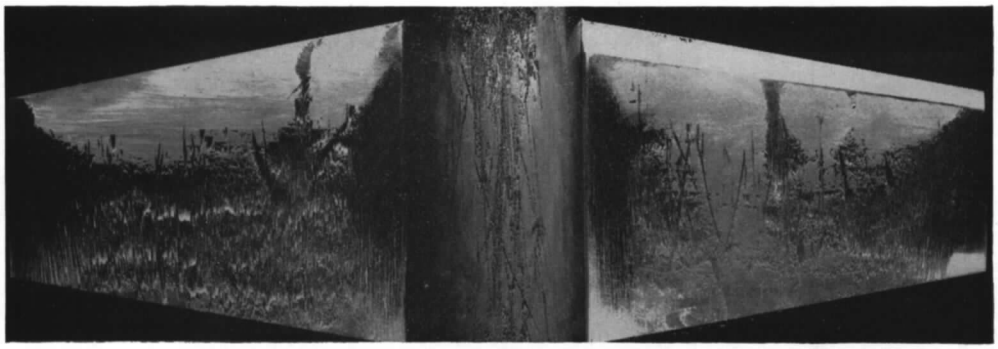

a. $\alpha = 4 \cdot 3°$

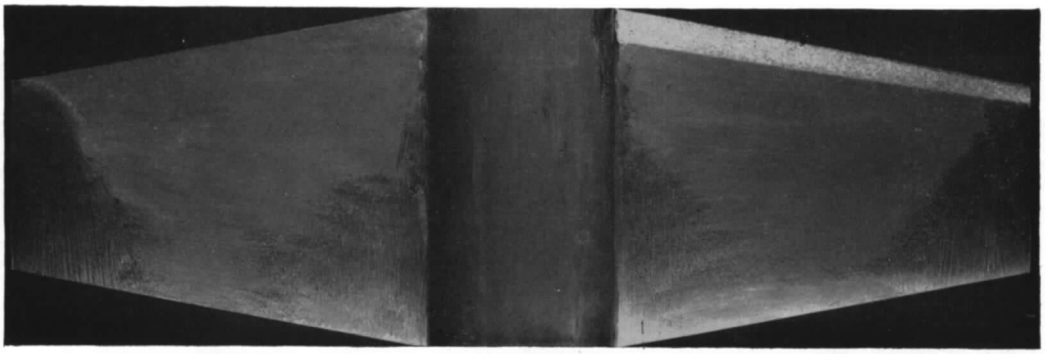

b. $\alpha = 6 \cdot 5°$

FIG. 6. Flow patterns on the wing at a Mach number of 0·70.

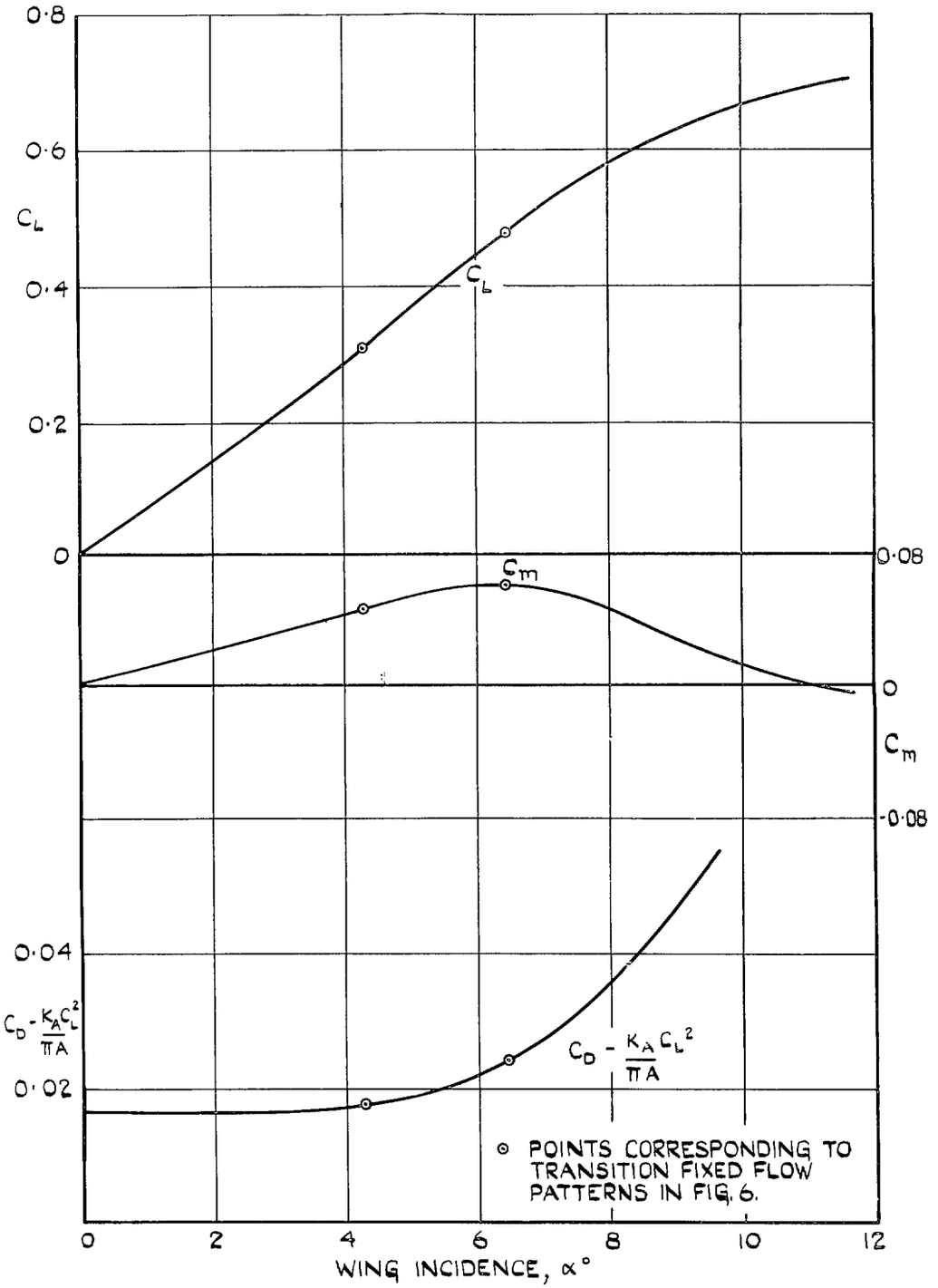

FIG. 7. The variation of C_L, C_m, and $C_D - (K_A/\pi A)C_L^2$ with incidence, α, at a Mach number of 0·70.

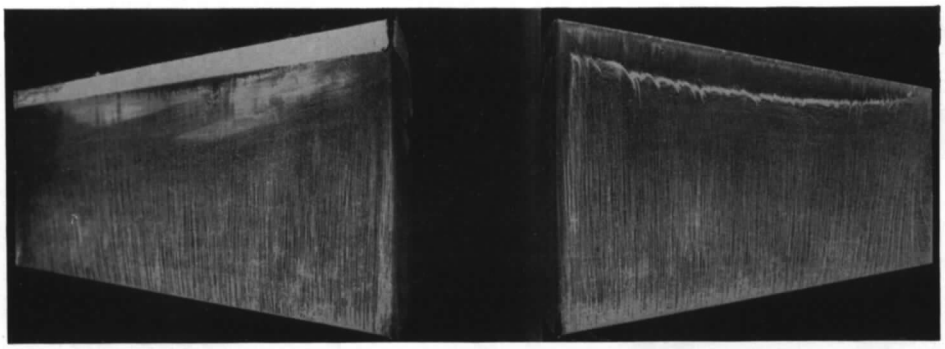

a. $\alpha = 4{\cdot}4°$

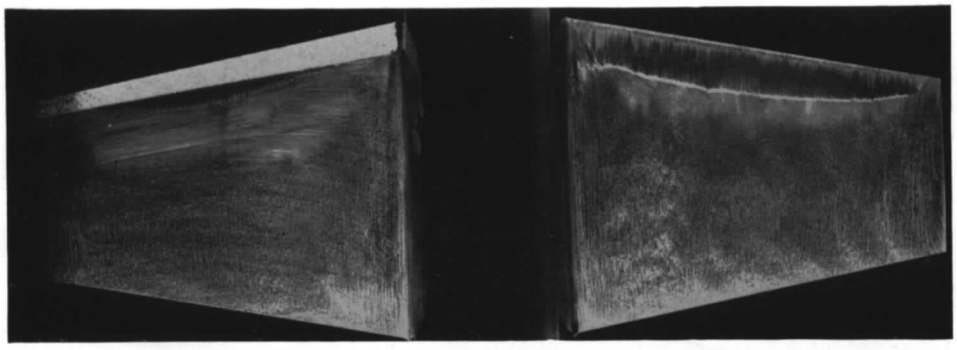

b. $\alpha = 5{\cdot}5°$

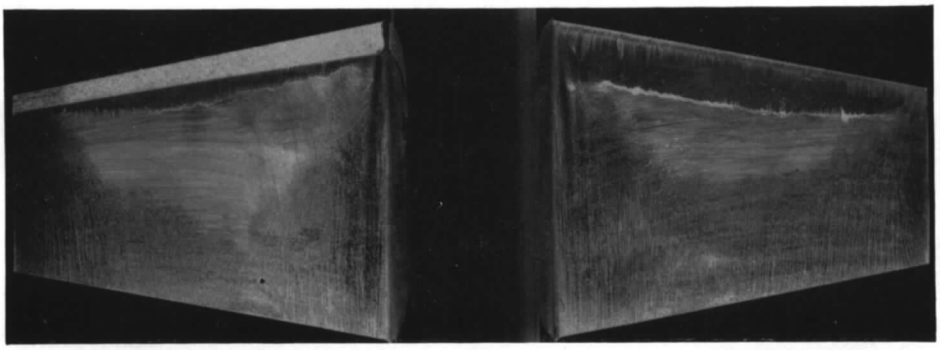

c. $\alpha = 6{\cdot}6°$

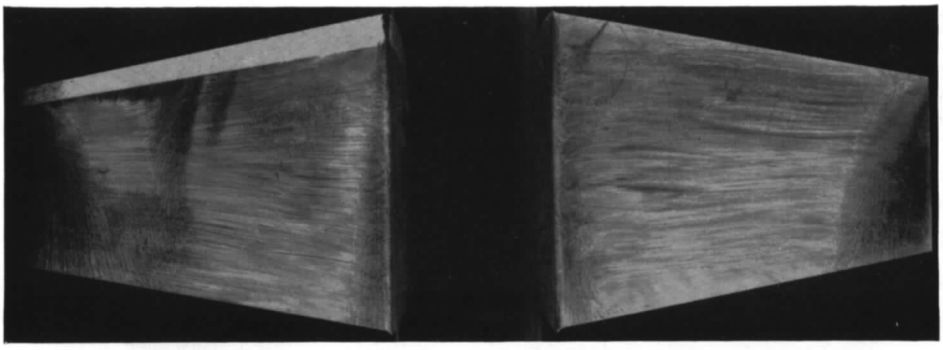

d. $\alpha = 7{\cdot}6°$

FIG. 8. Flow patterns on the wing at a Mach number of 0·80.

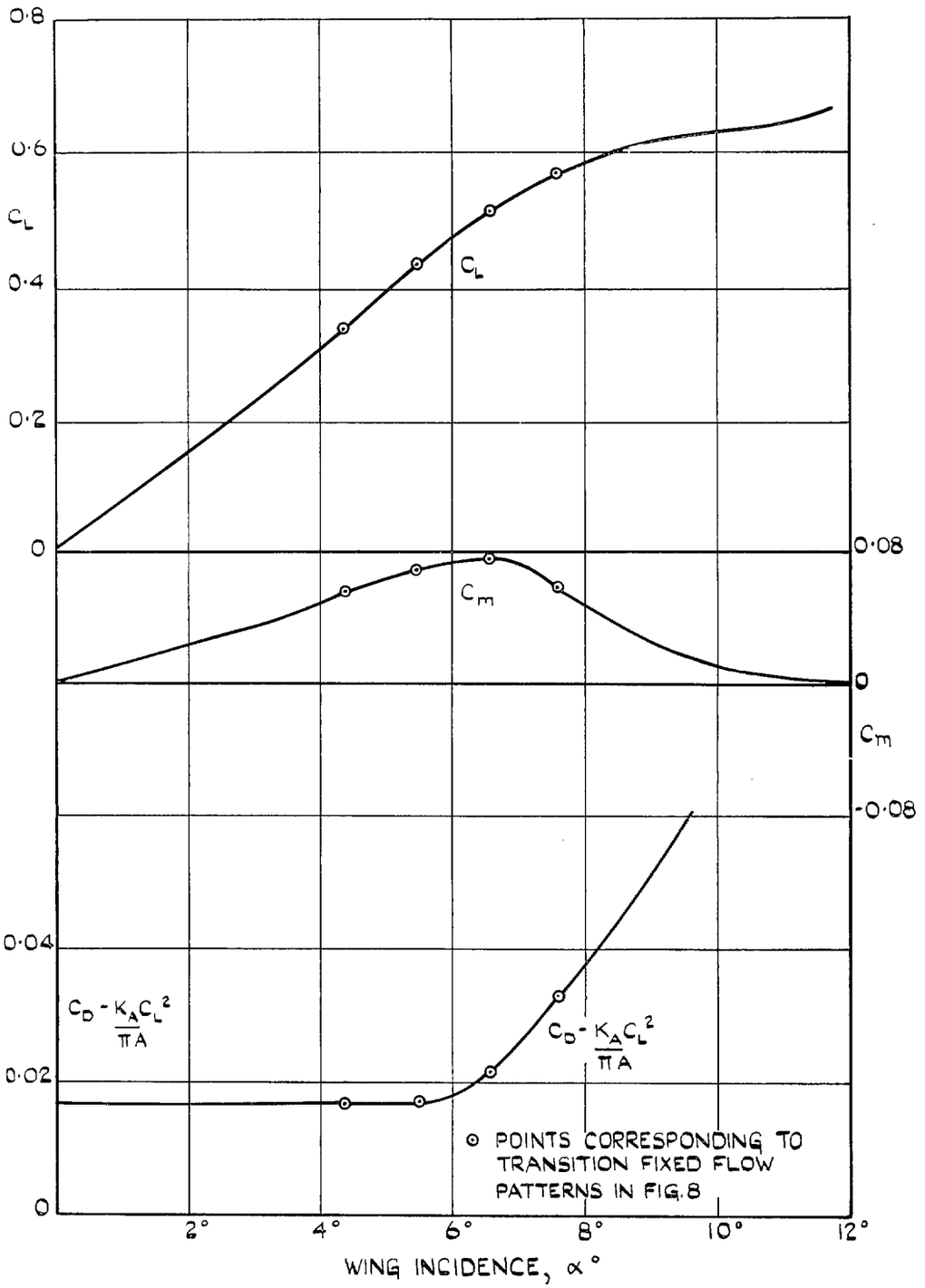

FIG. 9. The variation of C_L, C_m and $C_D - (K_A/\pi A)C_L^2$ with incidence, α, at a Mach number of 0·80.

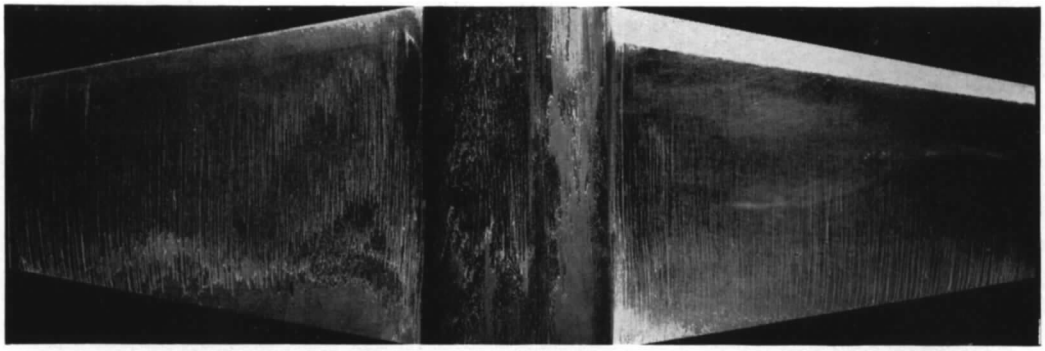

a. $\alpha = 0{\cdot}0°$

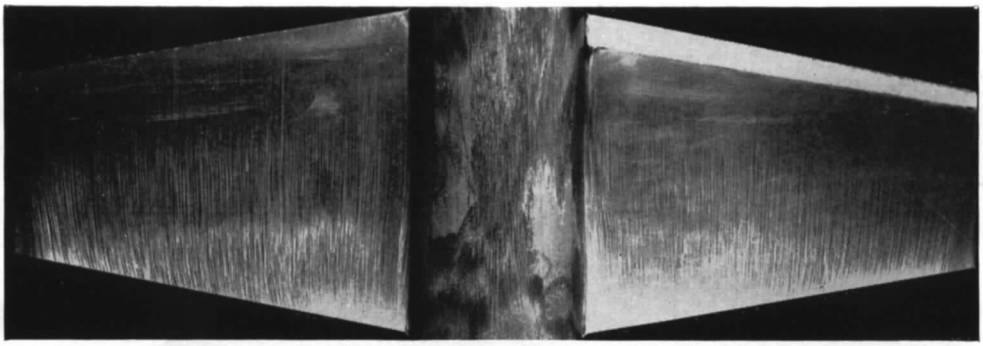

b. $\alpha = 2{\cdot}2°$

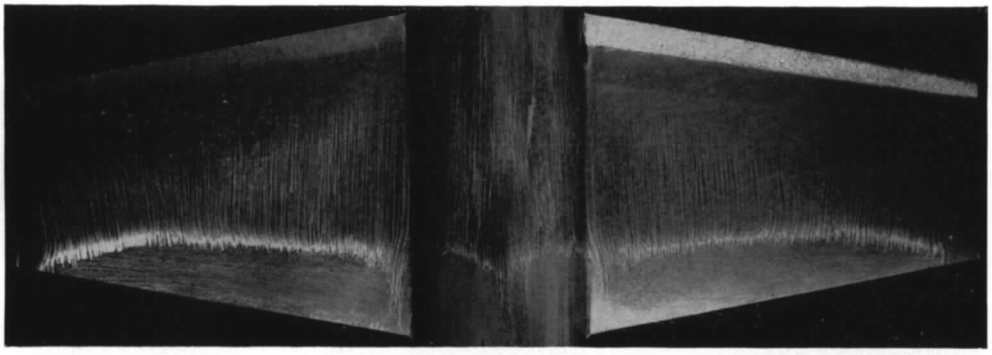

c. $\alpha = 4{\cdot}5°$

FIG. 10. Flow patterns on the wing at a Mach number of 0·93.

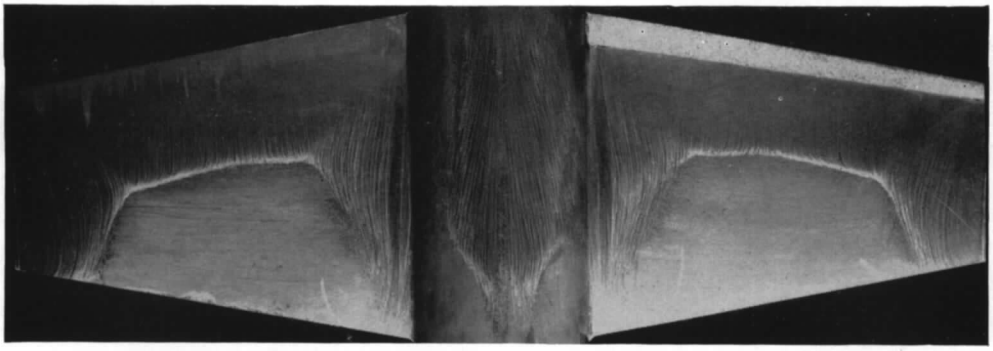

d. $\alpha = 8{\cdot}8°$

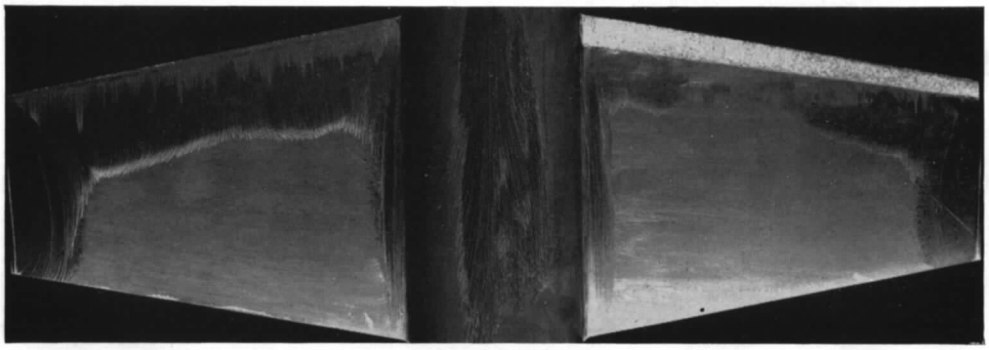

e. $\alpha = 11{\cdot}0°$

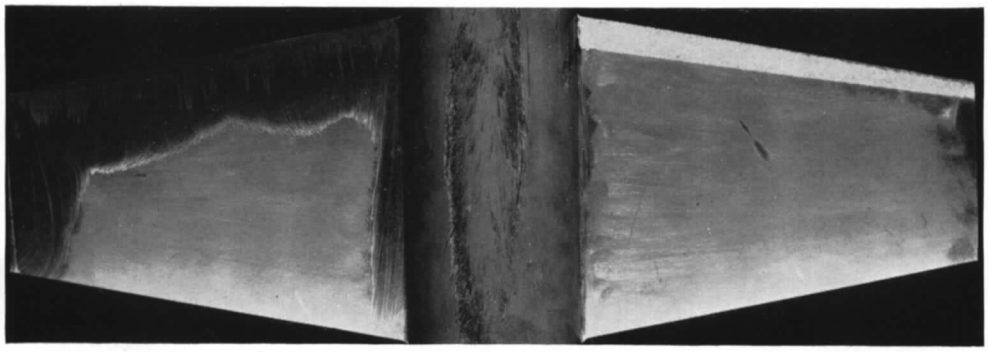

f. $\alpha = 11{\cdot}9°$

FIG. 10 contd. Flow patterns on the wing at a Mach number of 0·93.

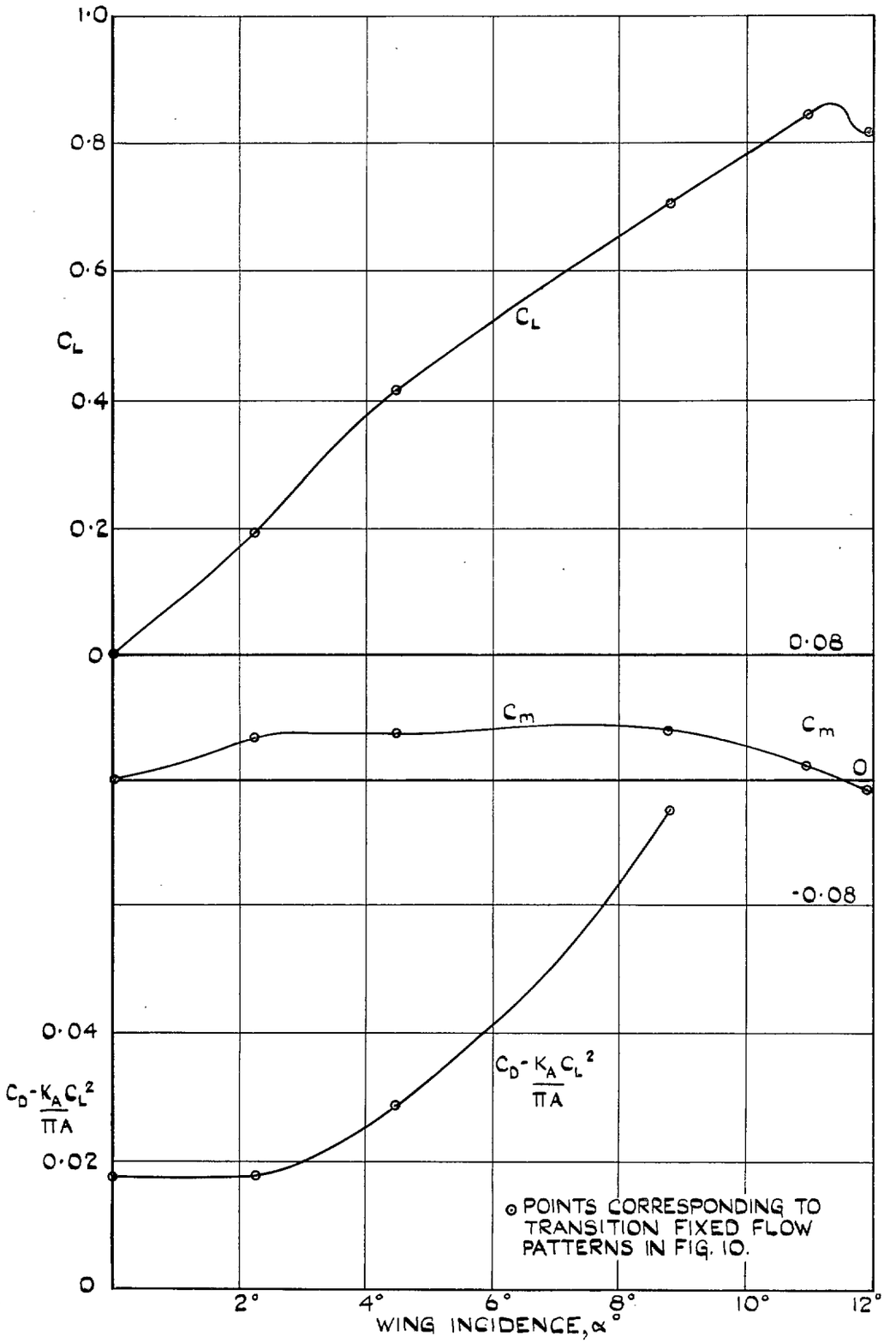

FIG. 11. The variation of C_L, C_m, and $C_D - (K_A/\pi A)C_L^2$ with incidence, α, at a Mach number of 0·93.

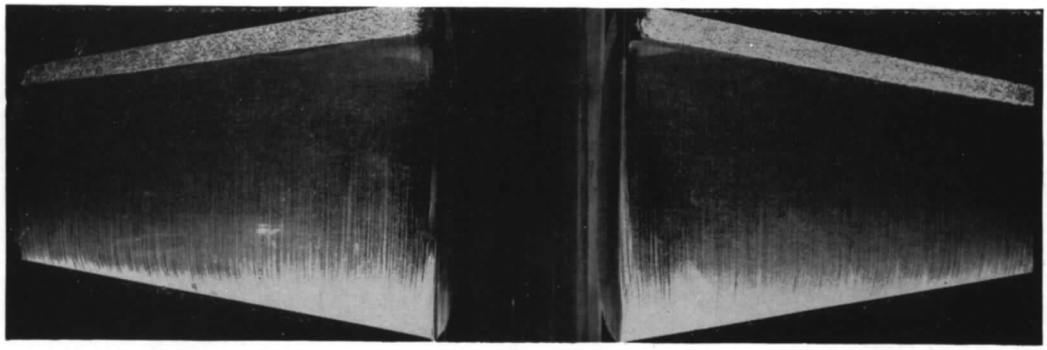

a. $\alpha = 0{\cdot}0°$

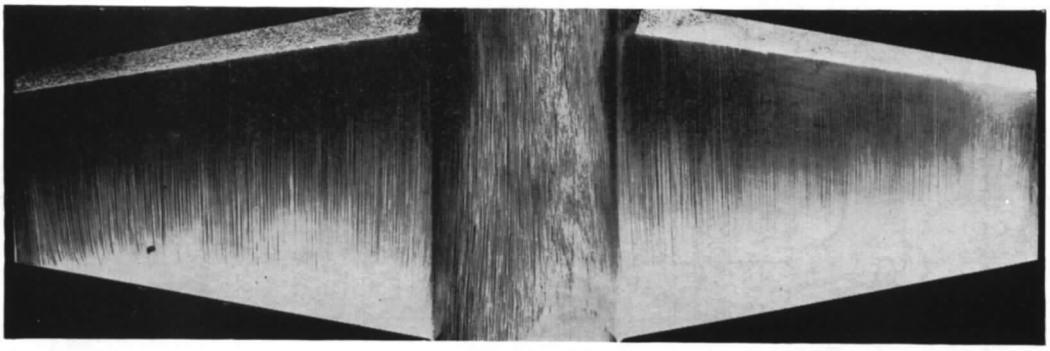

b. $\alpha = 2{\cdot}2°$

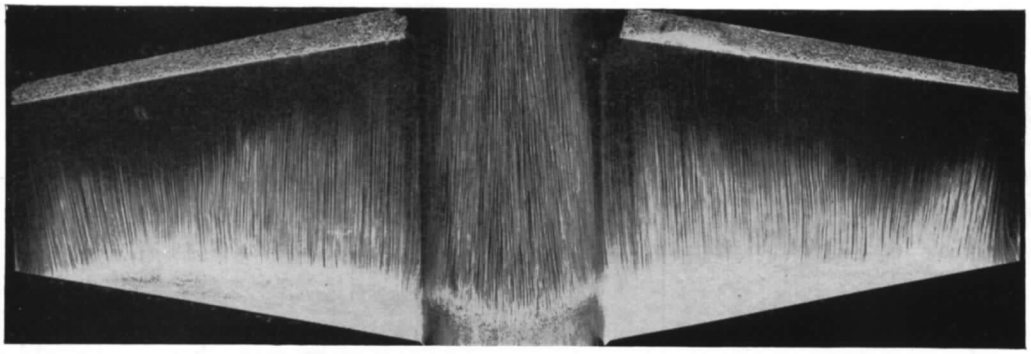

c. $\alpha = 4{\cdot}5°$

FIG. 12. Flow patterns on the wing at a Mach number of 0·96.

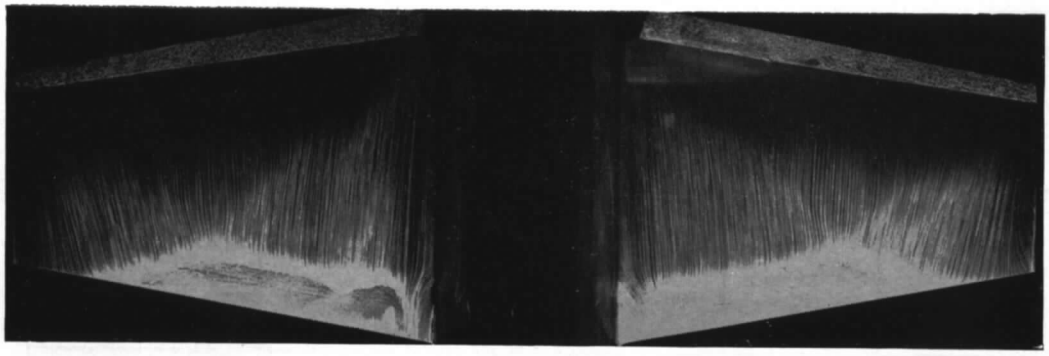

d. $\alpha = 6{\cdot}7°$

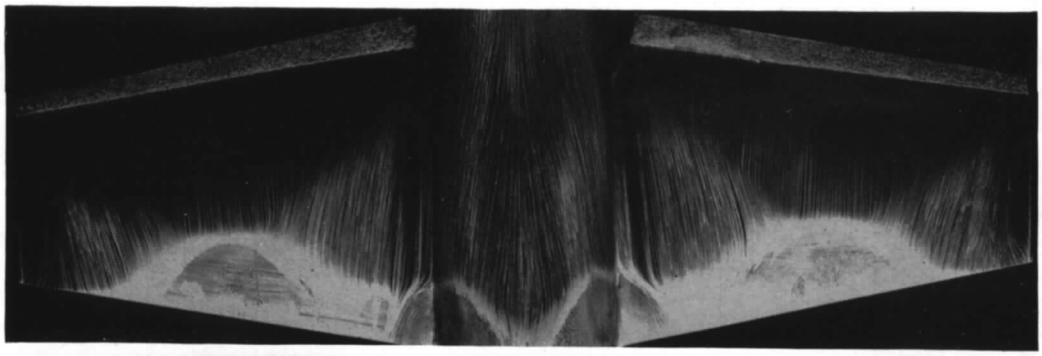

e. $\alpha = 8{\cdot}9°$

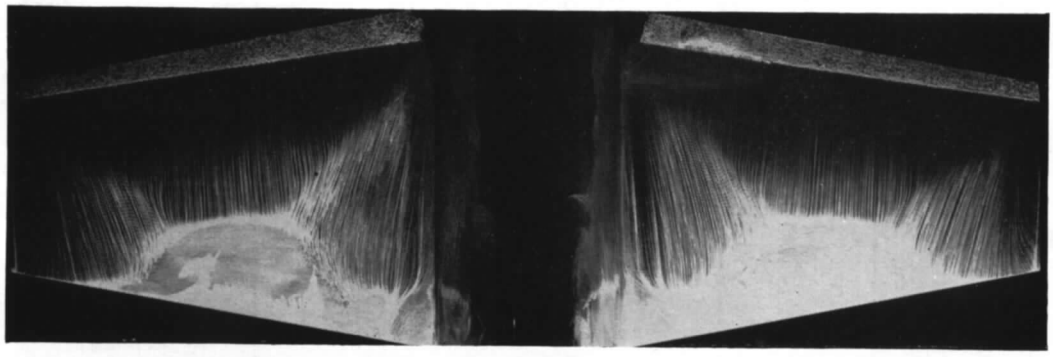

f. $\alpha = 10{\cdot}0°$

g. $\alpha = 12{\cdot}2°$

FIG. 12 contd. Flow patterns on the wing at a Mach number of 0·96.

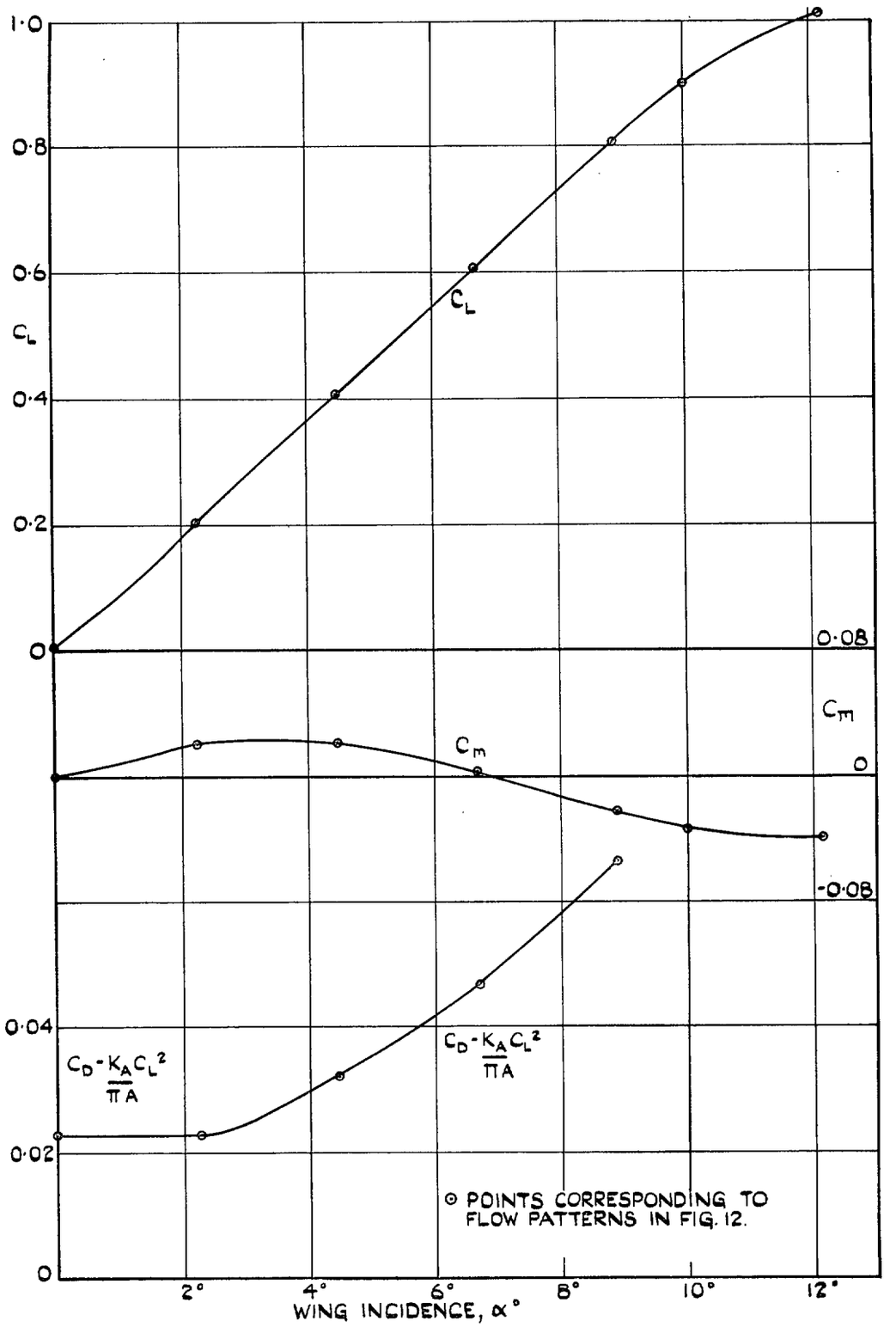

FIG. 13. The variation of C_L, C_m and $C_D - (K_A/\pi A)C_L^2$ with incidence, α, at a Mach number of 0·96.

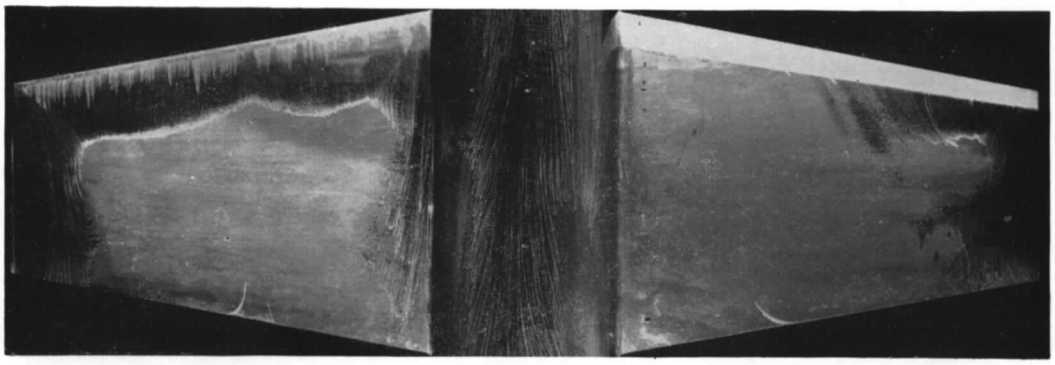

a. M = 0·85

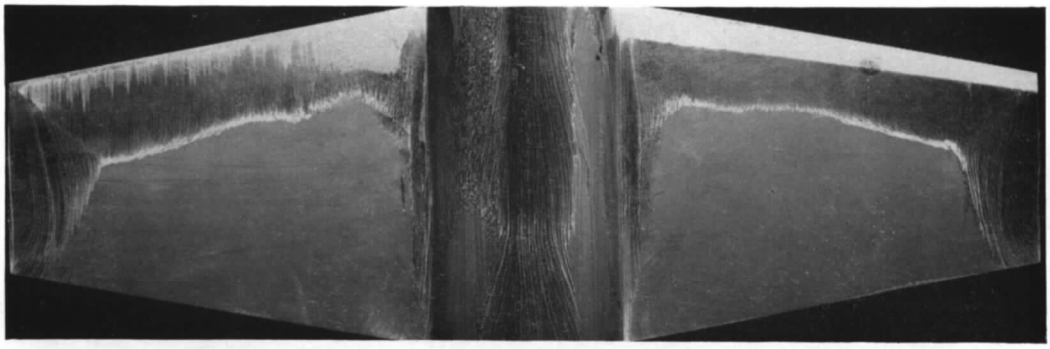

b. M = 0·90

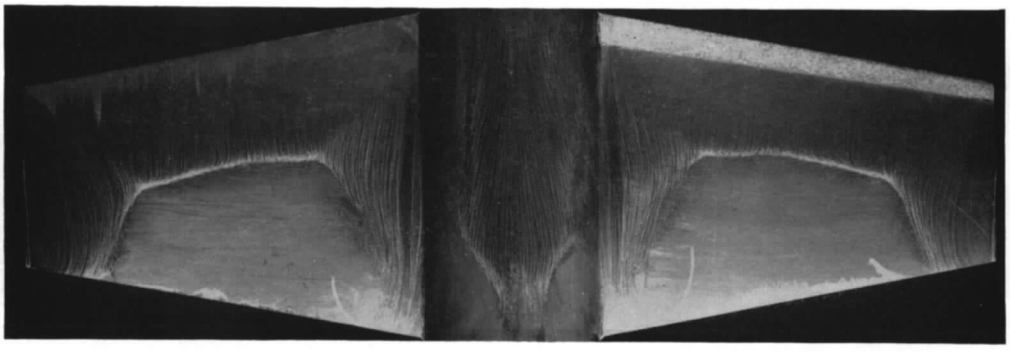

c. M = 0·93

FIG. 14. Flow patterns on the wing at 8·8 deg incidence, through the Mach number range.

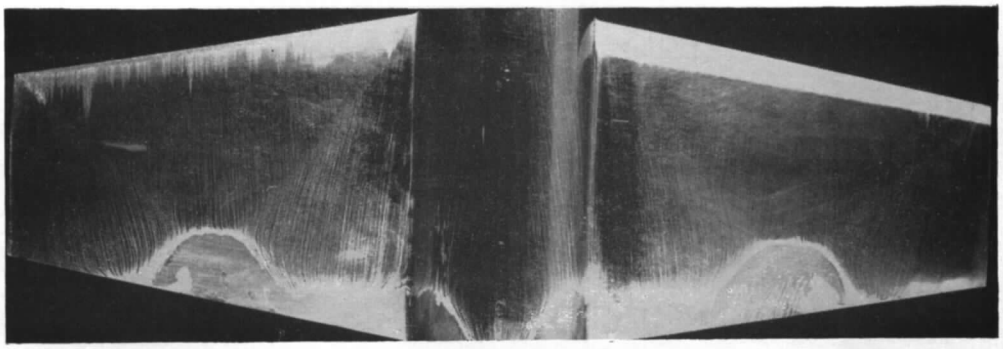

d. $M = 0{\cdot}96$

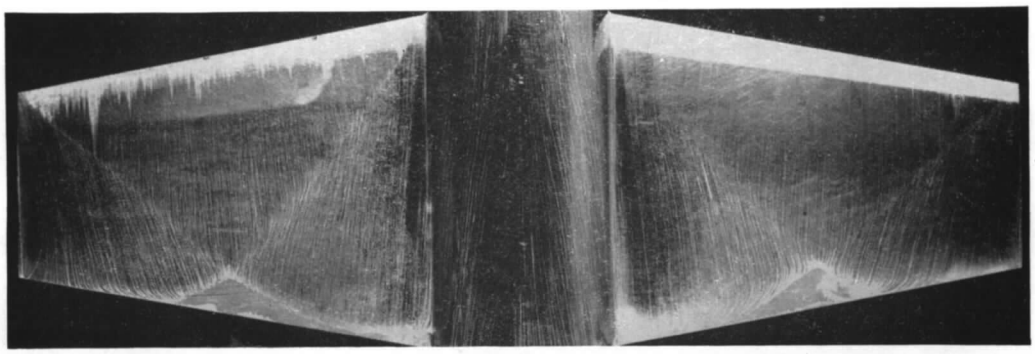

e. $M = 0{\cdot}99$

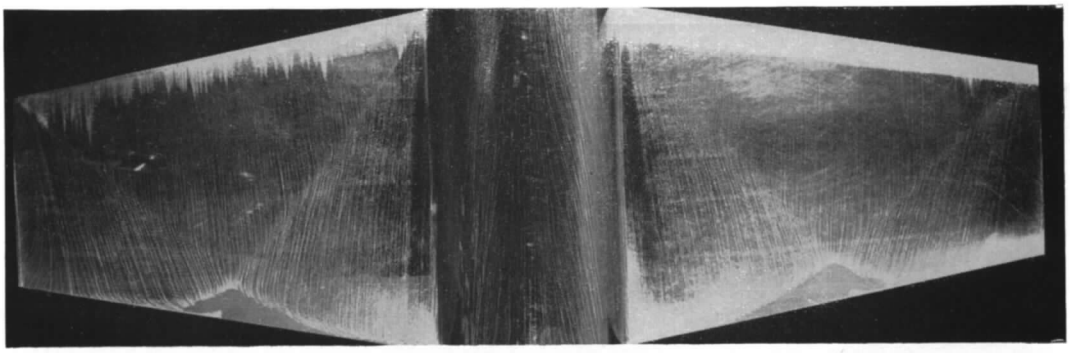

f. $M = 1{\cdot}02$

FIG. 14 contd. Flow patterns on the wing at 8·8 deg incidence, through the Mach number range.

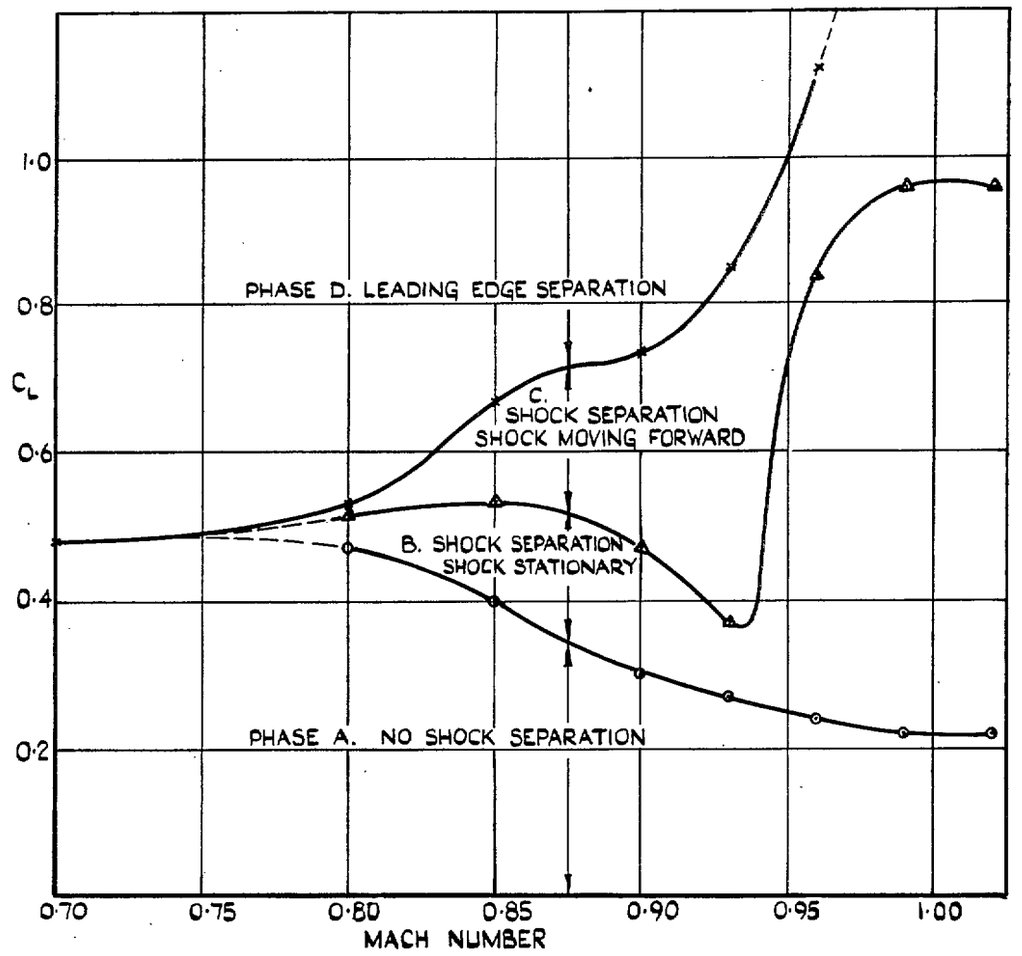

FIG. 15. The phase boundaries at transonic speeds.

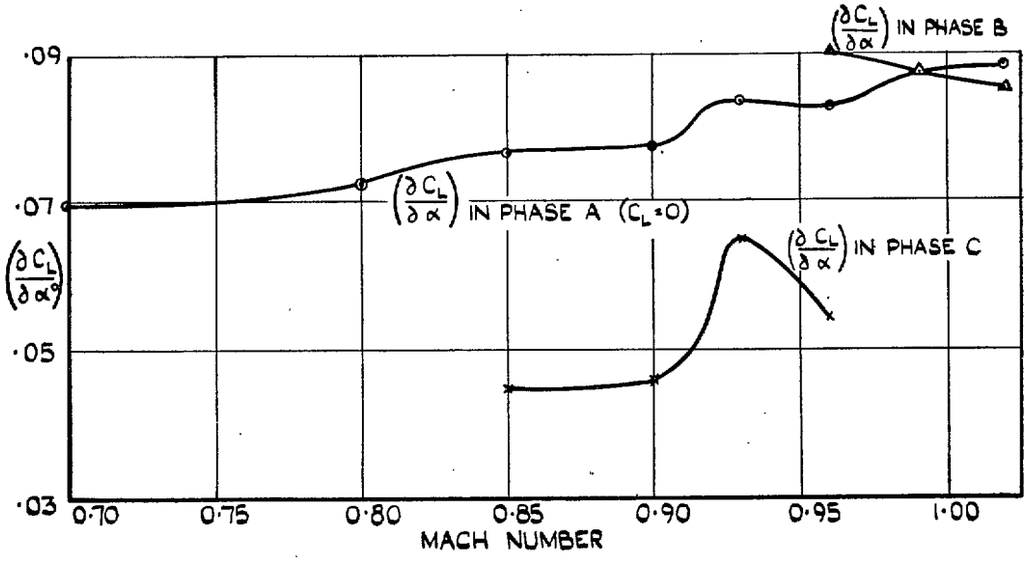

FIG. 16. The variation of the lift-curve slope, $\partial C_L/\partial \alpha_0$, with Mach number.

Publications of the Aeronautical Research Council

ANNUAL TECHNICAL REPORTS OF THE AERONAUTICAL RESEARCH COUNCIL (BOUND VOLUMES)

1939 Vol. I. Aerodynamics General, Performance, Airscrews, Engines. 50*s.* (52*s.*)
Vol. II. Stability and Control, Flutter and Vibration, Instruments, Structures, Seaplanes, etc. 63*s.* (65*s.*)

1940 Aero and Hydrodynamics, Aerofoils, Airscrews, Engines, Flutter, Icing, Stability and Control, Structures, and a miscellaneous section. 50*s.* (52*s.*)

1941 Aero and Hydrodynamics, Aerofoils, Airscrews, Engines, Flutter, Stability and Control, Structures. 63*s.* (65*s.* 3*d.*)

1942 Vol. I. Aero and Hydrodynamics, Aerofoils, Airscrews, Engines. 75*s.* (77*s.* 3*d.*)
Vol. II. Noise, Parachutes, Stability and Control, Structures, Vibration, Wind Tunnels. 47*s.* 6*d.* (49*s.* 3*d.*)

1943 Vol. I. Aerodynamics, Aerofoils, Airscrews. 80*s.* (82*s.*)
Vol. II. Engines, Flutter, Materials, Parachutes, Performance, Stability and Control, Structures. 90*s.* (92*s.* 3*d.*)

1944 Vol. I. Aero and Hydrodynamics, Aerofoils, Aircraft, Airscrews, Controls. 84*s.* (86*s.* 6*d.*)
Vol. II. Flutter and Vibration, Materials, Miscellaneous, Navigation, Parachutes, Performance, Plates and Panels, Stability, Structures, Test Equipment, Wind Tunnels. 84*s.* (86*s.* 6*d.*)

1945 Vol. I. Aero and Hydrodynamics, Aerofoils. 130*s.* (133*s.*)
Vol. II. Aircraft, Airscrews, Controls. 130*s.* (133*s.*)
Vol. III. Flutter and Vibration, Instruments, Miscellaneous, Parachutes, Plates and Panels, Propulsion. 130*s.* (132*s.* 9*d.*)
Vol. IV. Stability, Structures, Wind Tunnels, Wind Tunnel Technique. 130*s.* (132*s.* 9*d.*)

1946 Vol. I. Accidents, Aerodynamics, Aerofoils and Hydrofoils. 168*s.* (171*s.* 3*d.*)
Vol. II. Airscrews, Cabin Cooling, Chemical Hazards, Controls, Flames, Flutter, Helicopters, Instruments and Instrumentation, Interference, Jets, Miscellaneous, Parachutes. 168*s.* (170*s.* 9*d.*)
Vol. III. Performance, Propulsion, Seaplanes, Stability, Structures, Wind Tunnels. 168*s.* (171*s.*)

1947 Vol. I. Aerodynamics, Aerofoils, Aircraft. 168*s.* (171*s.* 3*d.*)
Vol. II. Airscrews and Rotors, Controls, Flutter, Materials, Miscellaneous, Parachutes, Propulsion, Seaplanes, Stability, Structures, Take-off and Landing. 168*s.* (171*s.* 3*d.*)

Annual Reports of the Aeronautical Research Council—

1939–48 3*s.* (3*s.* 5*d.*) 1949–54 5*s.* (5*s.* 5*d.*)

Index to all Reports and Memoranda published in the Annual Technical Reports, and separately—

April, 1950 - - - - R. & M. 2600 6*s.* (6*s.* 2*d.*)

Published Reports and Memoranda of the Aeronautical Research Council—

Between Nos. 2351–2449	R. & M. No. 2450	2*s.* (2*s.* 2*d.*)
Between Nos. 2451–2549	R. & M. No. 2550	2*s.* 6*d.* (2*s.* 8*d.*)
Between Nos. 2551–2649	R. & M. No. 2650	2*s.* 6*d.* (2*s.* 8*d.*)
Between Nos. 2651–2749	R. & M. No. 2750	2*s.* 6*d.* (2*s.* 8*d.*)
Between Nos. 2751–2849	R. & M. No. 2850	2*s.* 6*d.* (2*s.* 8*d.*)
Between Nos. 2851–2949	R. & M. No. 2950	3*s.* (3*s.* 2*d.*)
Between Nos. 2951–3049	R. & M. No. 3950	3*s.* 6*d.* (3*s.* 8*d.*)

Prices in brackets include postage

HER MAJESTY'S STATIONERY OFFICE

York House, Kingsway, London W.C.2; 423 Oxford Street, London W.1; 13a Castle Street, Edinburgh 2; 39 King Street, Manchester 2; 2 Edmund Street, Birmingham 3; 109 St. Mary Street, Cardiff; 50 Fairfax Street, Bristol 1; 80 Chichester Street, Belfast 1, *or through any bookseller.*

S.O. Code No. 23-3209